# PLY-THICKNESS AND PLY-BLOCK EFFECT ON FIBER/MATRIX INTERFACE CRACK GROWTH IN CROSS-PLY LAMINATES UNDER TENSILE LOADING

## INSIGHTS FROM LEFM-BASED MICROMECHANICAL MODELING

L. Di Stasio[1,2]

[1] Division of Materials Science, Luleå University of Technology, Luleå, Sweden
[2] EEIGM & IJL, Université de Lorraine, Nancy, France

Instituto IMDEA Materiales

Getafe, Madrid (ES) - September 17, 2019

# Outline

- Transverse Cracks Initiation
- Modeling
- Debond Initiation
- Debond Propagation
- Conclusions

# ↘ TRANSVERSE CRACKS INITIATION

# The Thin-ply "Advantage": new material

**2018**, $[45^\circ, 90^\circ, -45^\circ, 0^\circ]_{nS}$

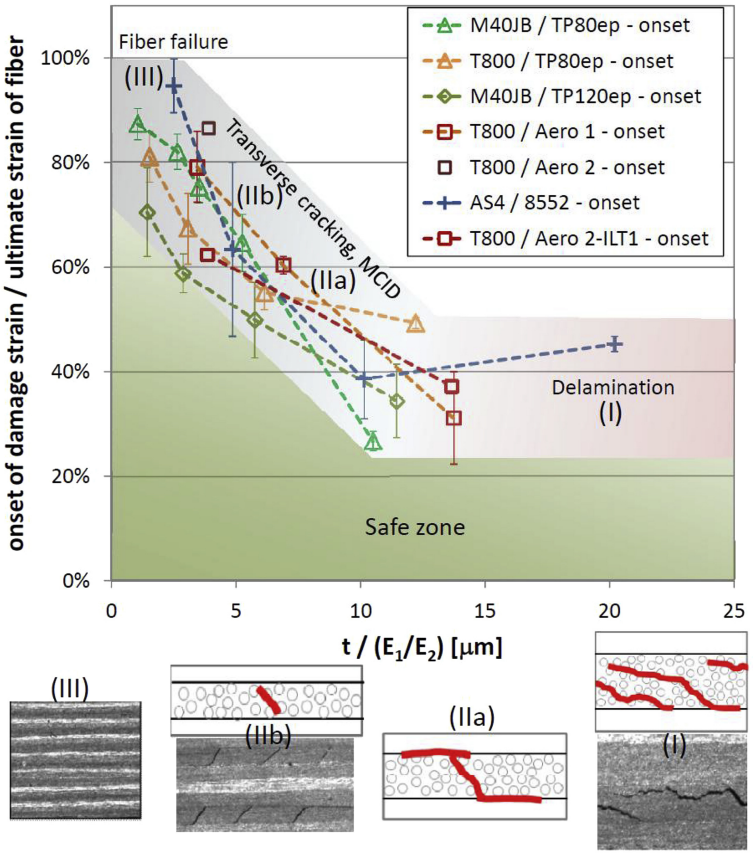


Cugnoni et al., Compos. Sci. Technol. **168**, 2018.

# The Thin-ply "Advantage": new material, old result

**2018**, $[45^\circ, 90^\circ, -45^\circ, 0^\circ]_{nS}$

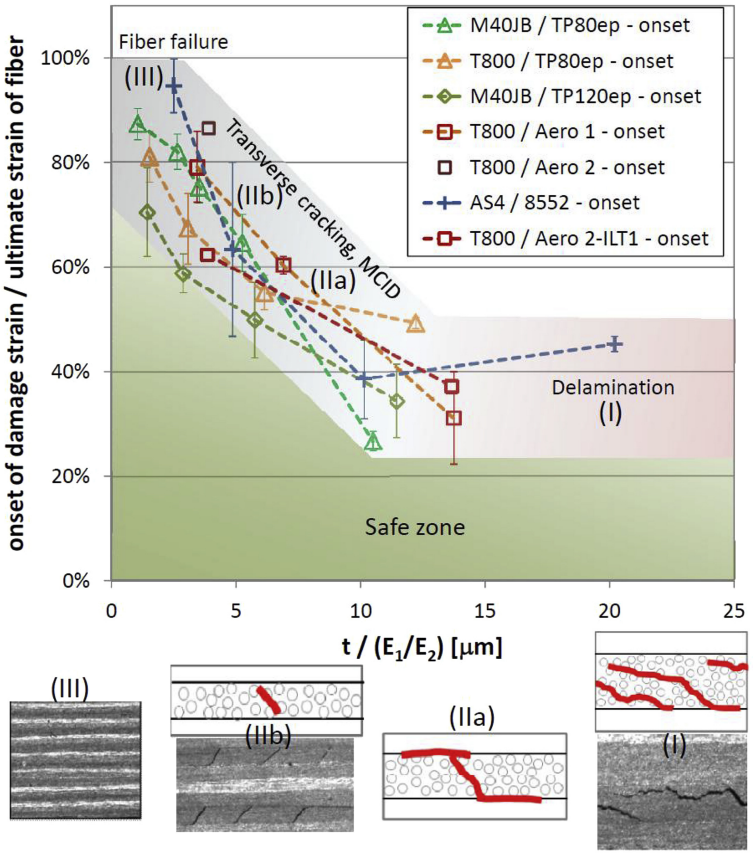


Cugnoni et al., Compos. Sci. Technol. **168**, 2018.

**1979**, $[0^\circ, 90^\circ_n]_S$

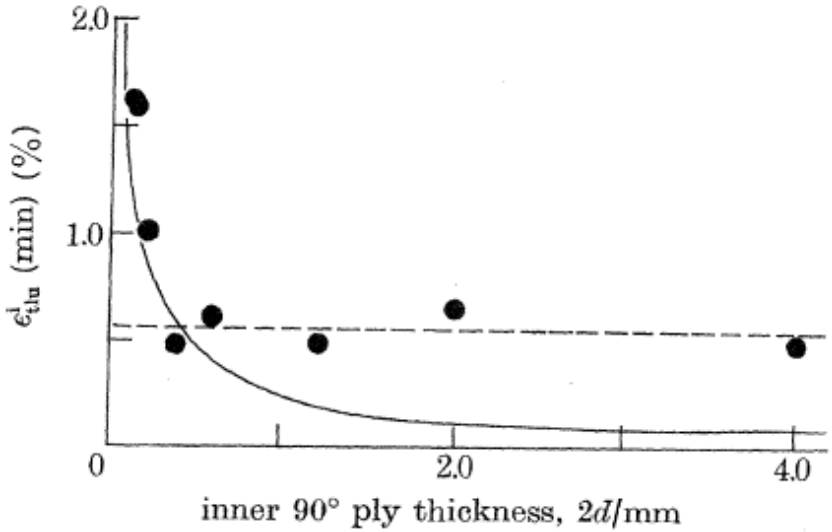


Bailey et al., P. Roy. Soc. A-Math. Phy. **366** (1727), 1979.

# The Thin-ply "Advantage": new material, old result?

**2018**, $[45^\circ, 90^\circ, -45^\circ, 0^\circ]_{nS}$

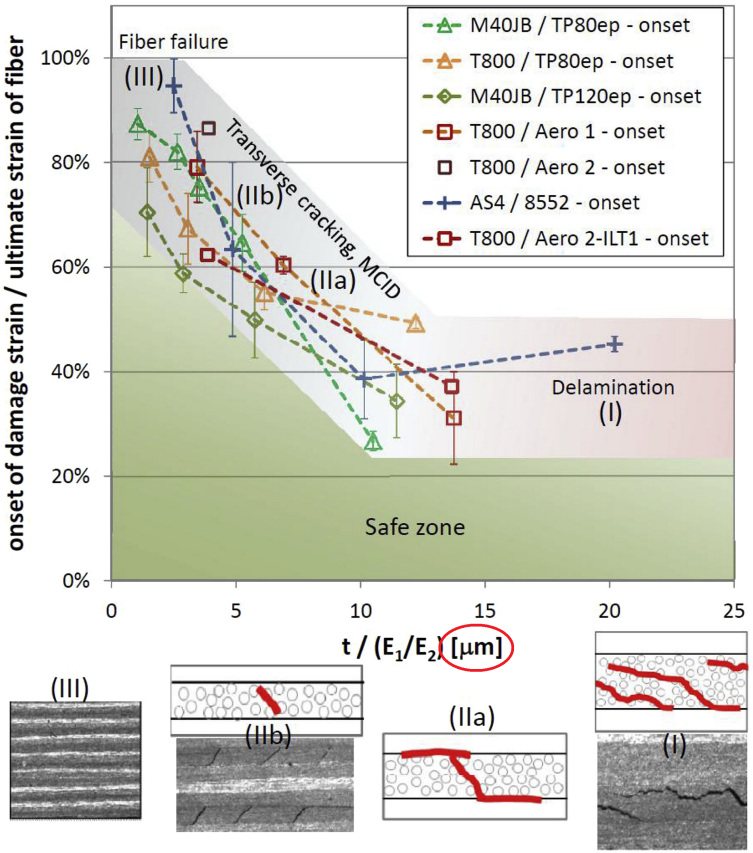


$t_{90^\circ} < 10 \varnothing_{fiber}$

Cugnoni et al., Compos. Sci. Technol. **168**, 2018.

**1979**, $[0^\circ, 90^\circ_n]_S$

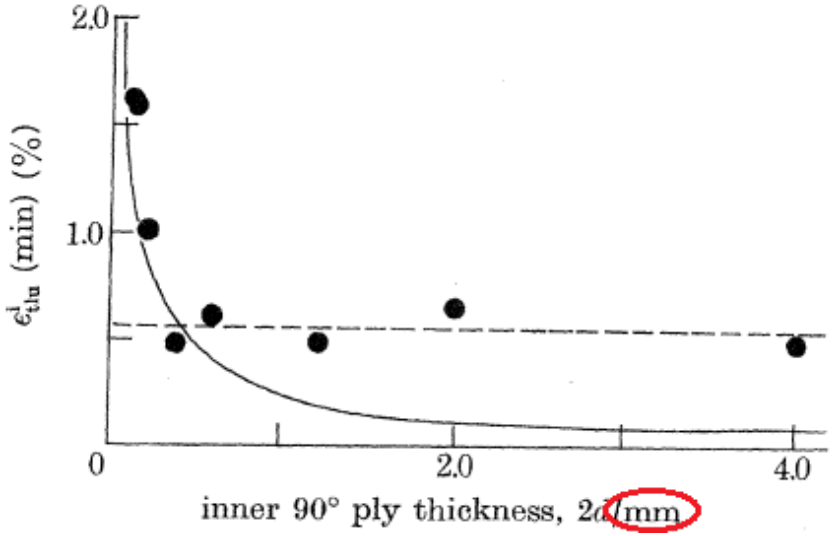


$t_{90^\circ} > 100 \varnothing_{fiber}$

Bailey et al., P. Roy. Soc. A-Math. Phy. **366** (1727), 1979.

# Micromechanics of Initiation

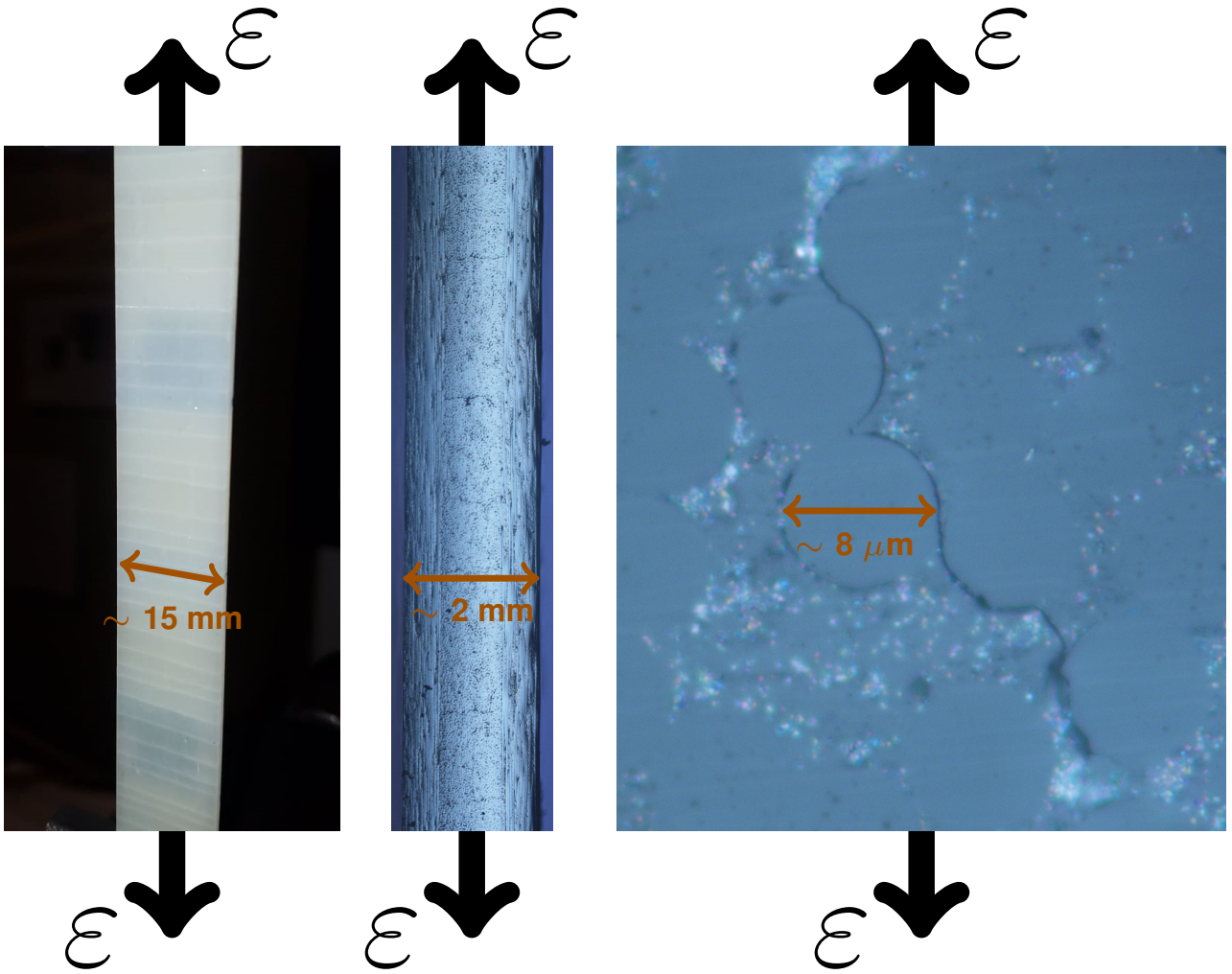


**Left:**
front view of $[0, 90_2]_S$, visual inspection.

**Center:**
edge view of $[0, 90]_S$, optical microscope.

**Right:**
edge view of $[0, 90]_S$, optical microscope.

# Micromechanics of Initiation

## Stage 1: isolated debonds

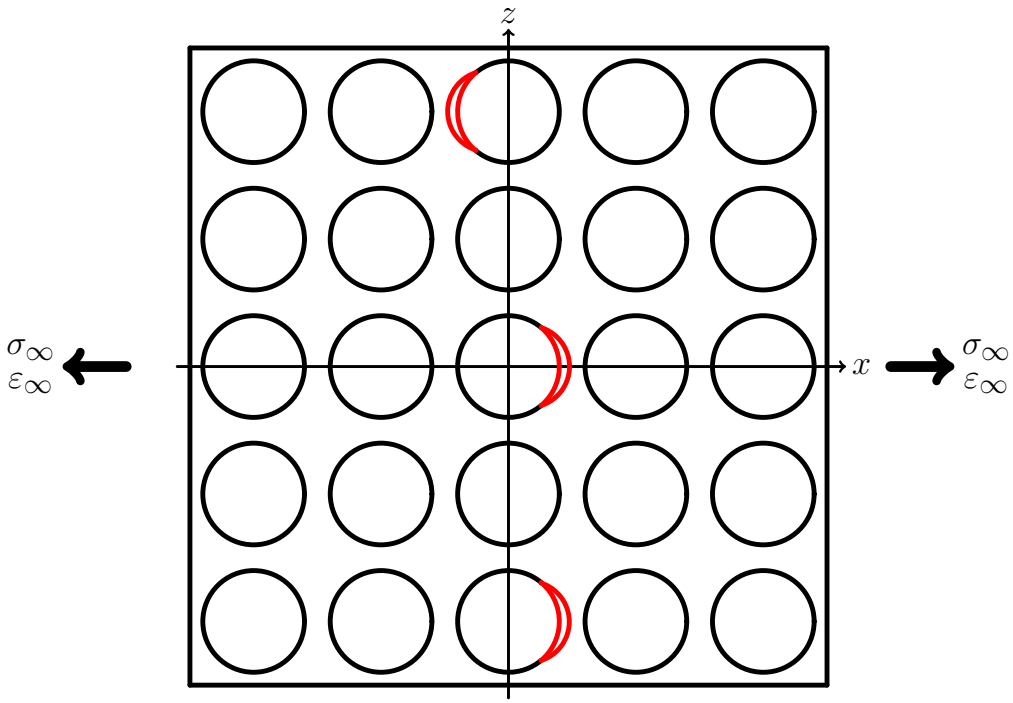


Bailey et al., P. Roy. Soc. A-Math. Phy. **366** (1727), 1979.

Bailey et al., J. Mater. Sci. **16** (3), 1981.

Zhang et al., Compos. Part A-Appl. S. **28** (4), 1997.

# Micromechanics of Initiation

## Stage 2: consecutive debonds

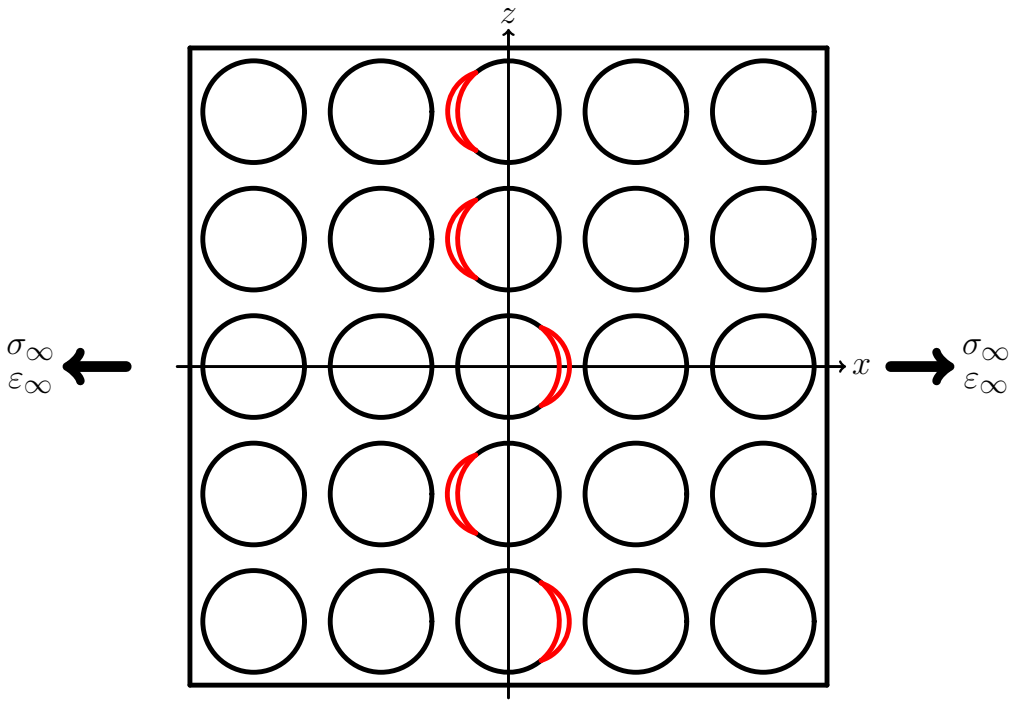


Bailey et al., P. Roy. Soc. A-Math. Phy. **366** (1727), 1979.

Bailey et al., J. Mater. Sci. **16** (3), 1981.

Zhang et al., Compos. Part A-Appl. S. **28** (4), 1997.

# Micromechanics of Initiation

## Stage 3: kinking

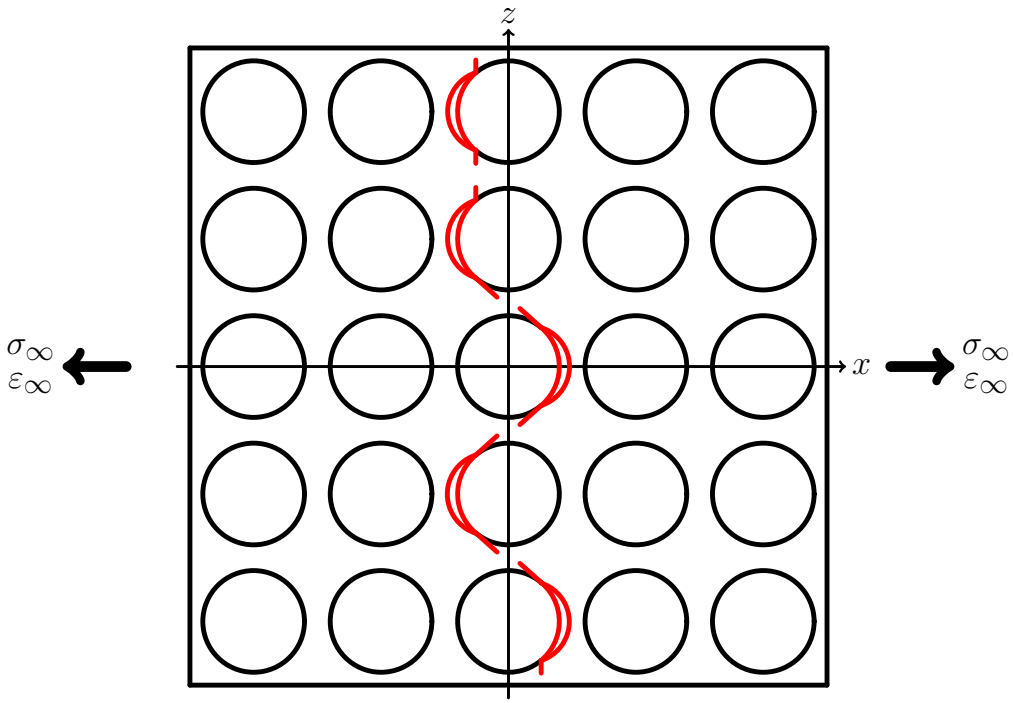


Bailey et al., P. Roy. Soc. A-Math. Phy. **366** (1727), 1979.

Bailey et al., J. Mater. Sci. **16** (3), 1981.

Zhang et al., Compos. Part A-Appl. S. **28** (4), 1997.

# Micromechanics of Initiation

## Stage 4: coalescence

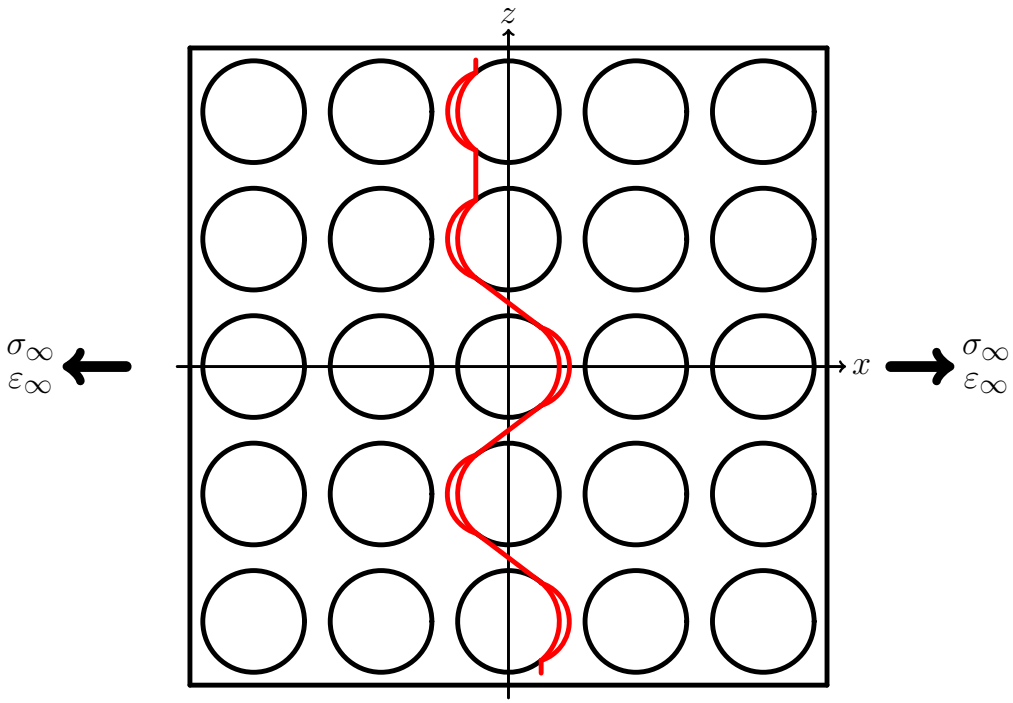


Bailey et al., P. Roy. Soc. A-Math. Phy. **366** (1727), 1979.

Bailey et al., J. Mater. Sci. **16** (3), 1981.

Zhang et al., Compos. Part A-Appl. S. **28** (4), 1997.

# A Counter-intuitive Observation

$$[\mathbf{0}^\circ, \mathbf{90}^\circ_\mathbf{n}]_\mathbf{S}$$

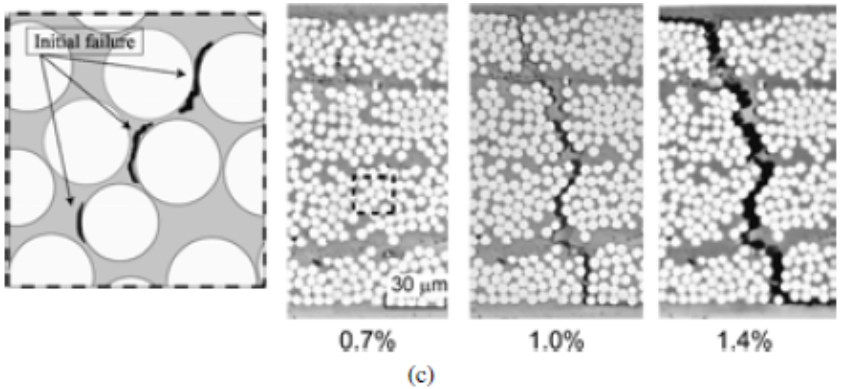


$n = 4$, $t_{90^\circ} = 160\mu m$

Saito et al., Adv. Compos. Mater. **21** (1), 2012.

# A Counter-intuitive Observation

$$[\mathbf{0}^\circ, \mathbf{90}^\circ_\mathbf{n}]_\mathbf{S}$$

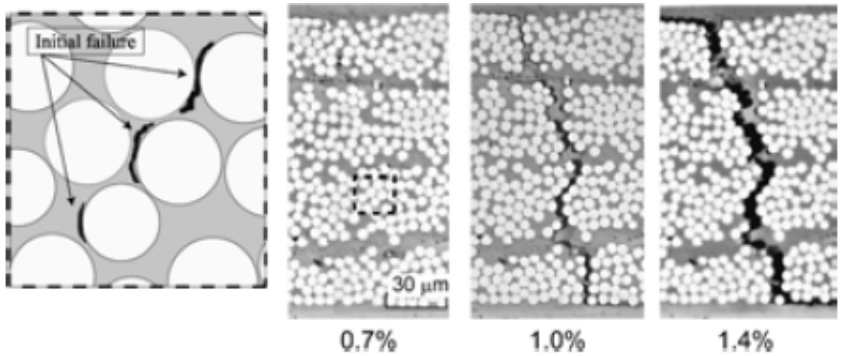


$n = 4$, $t_{90^\circ} = 160\mu m$

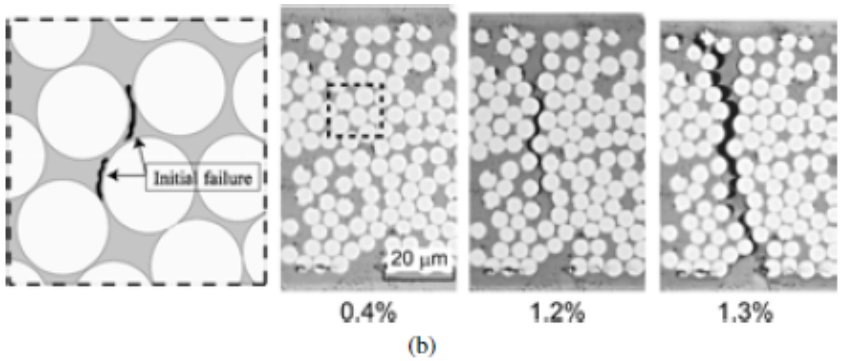


$n = 2$, $t_{90^\circ} = 80\mu m$

Saito et al., Adv. Compos. Mater. **21** (1), 2012.

# A Counter-intuitive Observation

$$[0^\circ, 90^\circ_n]_S$$

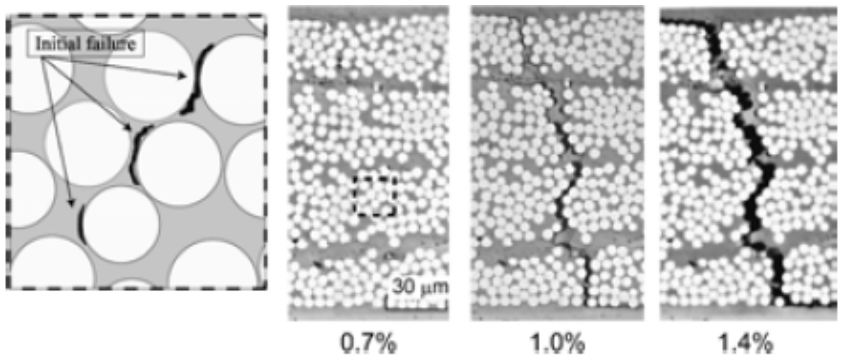


$n = 4$, $t_{90^\circ} = 160\mu m$

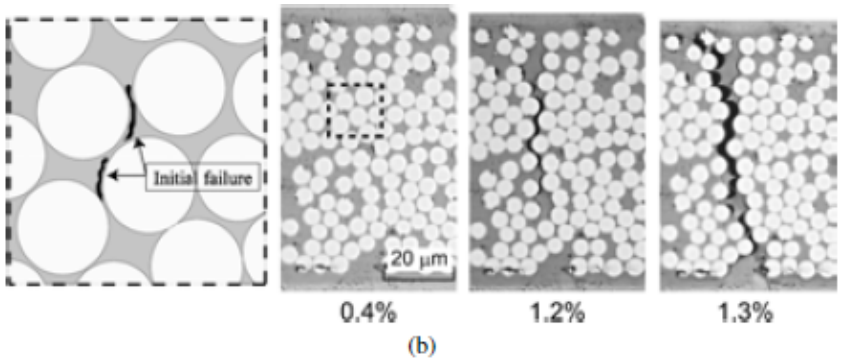


$n = 2$, $t_{90^\circ} = 80\mu m$

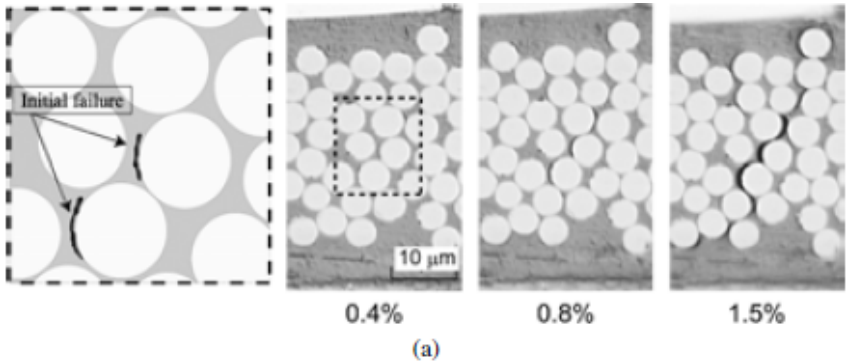


$n = 1$, $t_{90^\circ} = 40\mu m$

Saito et al., Adv. Compos. Mater. **21** (1), 2012.

# Objectives

Can we talk about a ply-thickness effect for the fiber-matrix interface crack?

**Stage 1: isolated debonds**

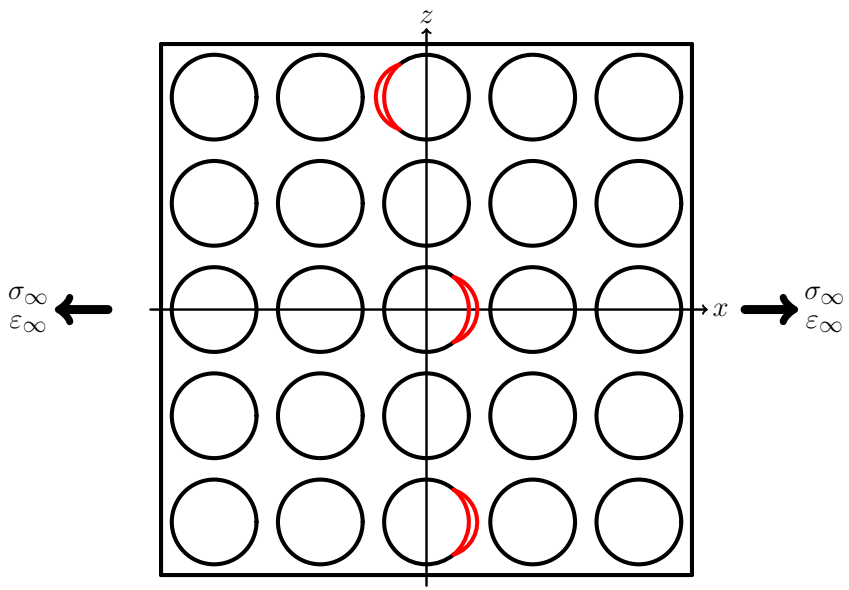

# ↘ MODELING

# Geometry

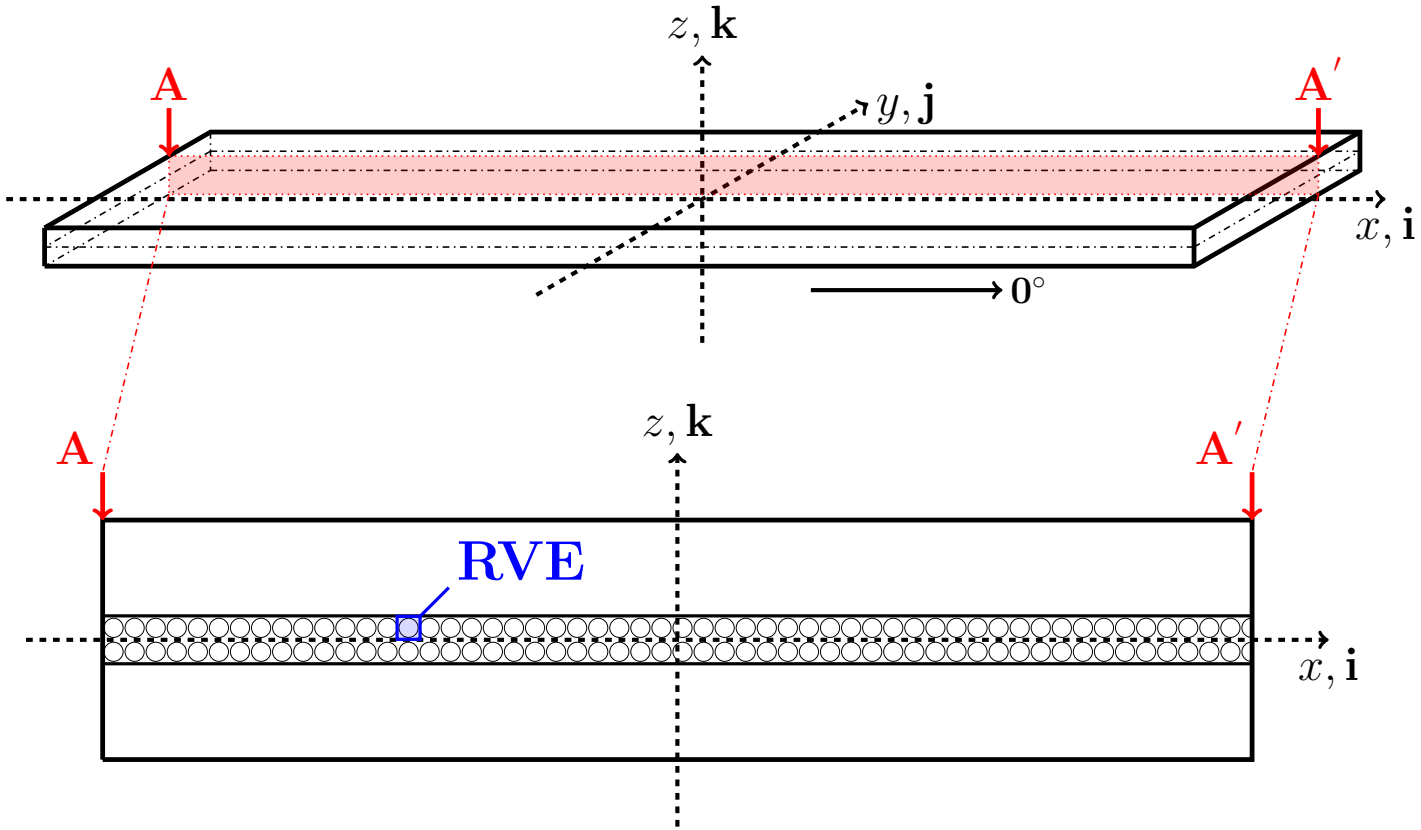


- ➔ $L, W >> t$
- ➔ $L, W \to \infty$
- ➔ Square packing
- ➔ $L_d >> \Delta\theta_d$
- ➔ 2D RVE

# Representative Volume Elements

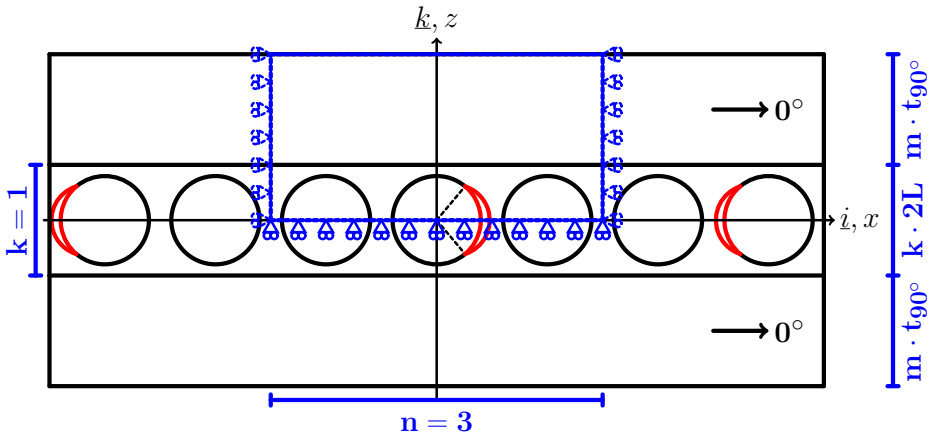


$$n \times 1 - m \cdot t_{90^\circ}$$

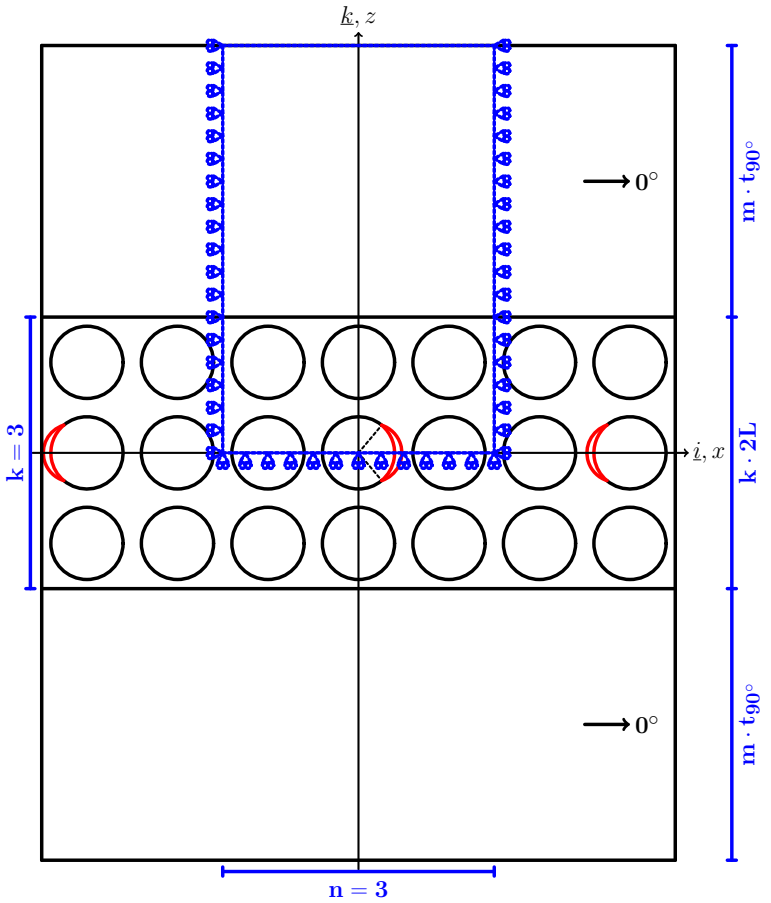


$$n \times k - m \cdot t_{90^\circ}$$

# Representative Volume Elements

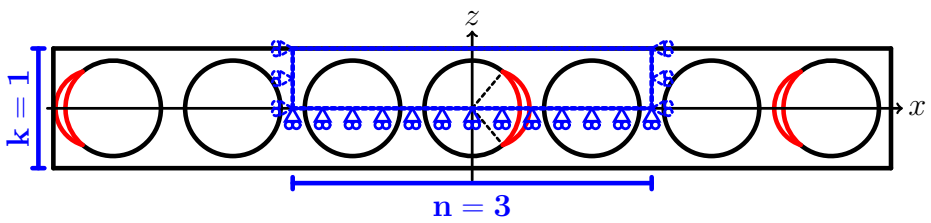


- *free*
- $n \times 1$ – *coupling*
- *coupling* + *H*

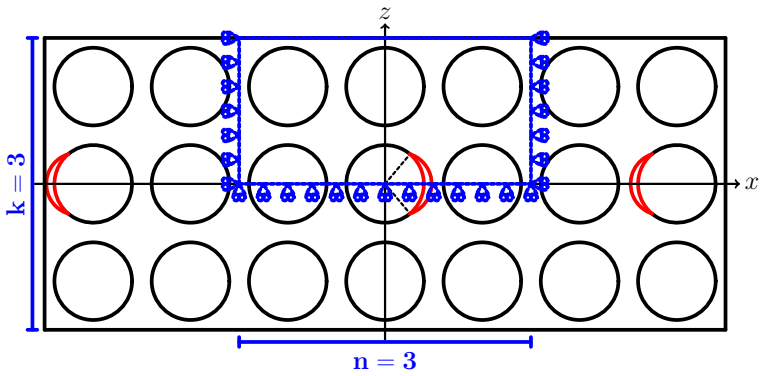


- *free*
- $n \times k$ – *coupling*
- *coupling* + *H*

# Assumptions

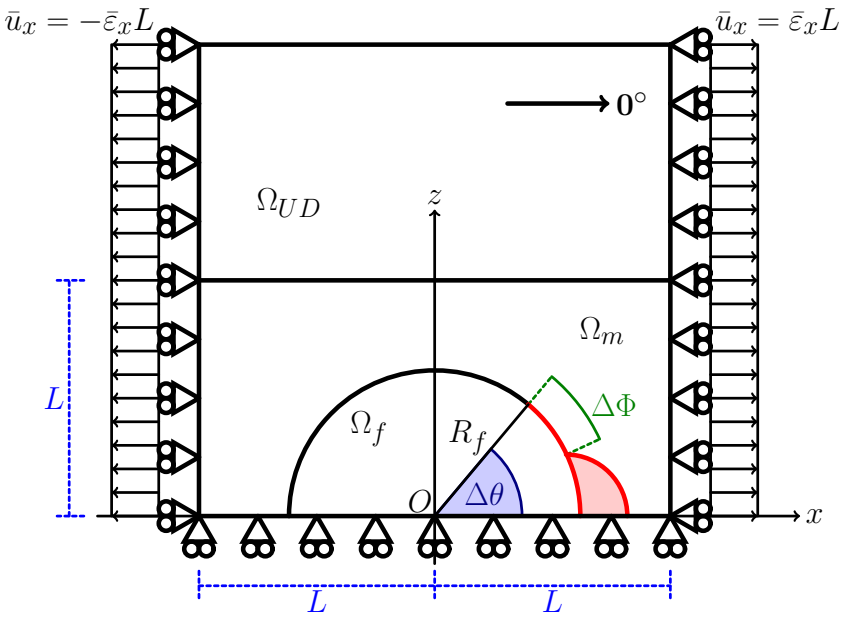


$$R_f = 1 \ [\mu m] \quad L = \frac{R_f}{2}\sqrt{\frac{\pi}{V_f}}$$

- ➔ Linear elastic, homogeneous materials
- ➔ Concentric Cylinders Assembly with Self-Consistent Shear Model for UD
- ➔ Plane strain
- ➔ Frictionless contact interaction
- ➔ Symmetric w.r.t. x-axis
- ➔ Coupling of x-displacements on left and right side (repeating unit cell)
- ➔ Applied uniaxial tensile strain $\bar{\varepsilon}_x = 1\%$
- ➔ $V_f = 60\%$

| **Material** | $V_f$ [%] | $E_L$ [GPa] | $E_T$ [GPa] | $\mu_{LT}$ [GPa] | $\nu_{LT}$ [−] | $\nu_{TT}$ [−] |
|---|---|---|---|---|---|---|
| Glass fiber | - | 70.0 | 70.0 | 29.2 | 0.2 | 0.2 |
| Epoxy | - | 3.5 | 3.5 | 1.25 | 0.4 | 0.4 |
| UD | 60.0 | 43.442 | 13.714 | 4.315 | 0.273 | 0.465 |

# Solution

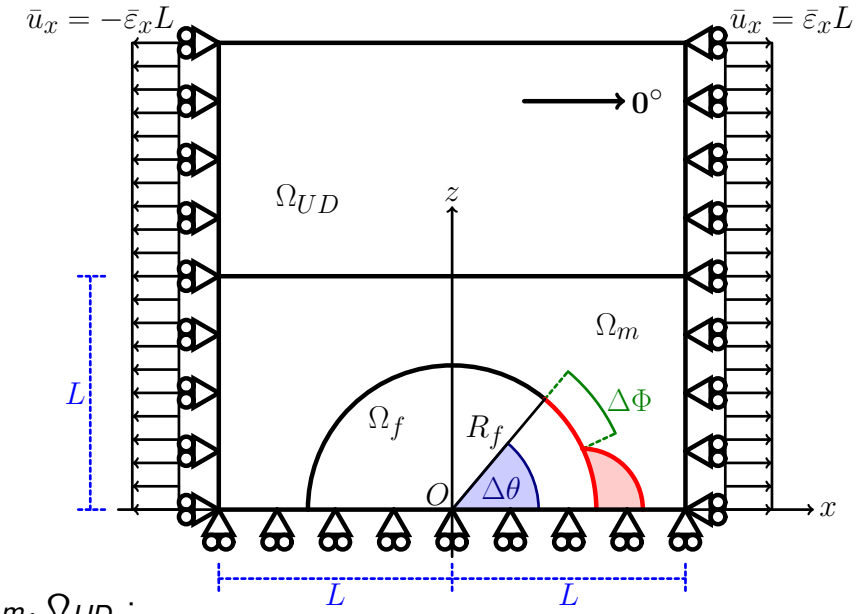


in $\Omega_f, \Omega_m, \Omega_{UD}$ :

$$\frac{\partial^2 \varepsilon_{xx}}{\partial z^2} + \frac{\partial^2 \varepsilon_{zz}}{\partial x^2} = \frac{\partial^2 \gamma_{zx}}{\partial x \partial z}$$

$$\varepsilon_y = \gamma_{xy} = \gamma_{yz} = 0$$

$$\frac{\partial \sigma_{xx}}{\partial x} + \frac{\partial \tau_{zx}}{\partial z} = 0$$

$$\frac{\partial \tau_{zx}}{\partial x} + \frac{\partial \sigma_{zz}}{\partial z} = 0$$

$$\sigma_{yy} = \nu \left( \sigma_{xx} + \sigma_{zz} \right)$$

for $0° \leq \alpha \leq \Delta\theta$ :

$$\left( \vec{u}_m \left( R_f, \alpha \right) - \vec{u}_f \left( R_f, \alpha \right) \right) \cdot \vec{n}_\alpha \geq 0$$

for $\Delta\theta \leq \alpha \leq 180°$ :

$$\vec{u}_m \left( R_f, \alpha \right) - \vec{u}_f \left( R_f, \alpha \right) = 0$$

$$\sigma_{ij} = E_{ijkl} \varepsilon_{kl}$$

$$+ BC$$

- ➔ Oscillating singularity

$$\sigma \sim r^{-\frac{1}{2}} \sin\left( \varepsilon \log r \right), \quad V_f \to 0$$

$$\varepsilon = \frac{1}{2\pi} \log\left( \frac{1-\beta}{1+\beta} \right)$$

$$\beta = \frac{\mu_2 \left( \kappa_1 - 1 \right) - \mu_1 \left( \kappa_2 - 1 \right)}{\mu_2 \left( \kappa_1 + 1 \right) + \mu_1 \left( \kappa_2 + 1 \right)}$$

- ➔ receding contact
- ➔ Finite Element Method (FEM) in Abaqus™
- ➔ $2^{nd}$ order shape functions
- ➔ 6-nodes triangles & 8-nodes quadrilaterals
- ➔ regular mesh of quadrilaterals at the crack tip:
  - $AR \sim 1$
  - $\delta = 0.05°$

# ↘ Debond Initiation

# $\sigma_{rr}$ vs $\tau_{r\theta}$: radial stress vs tangential shear at the interface

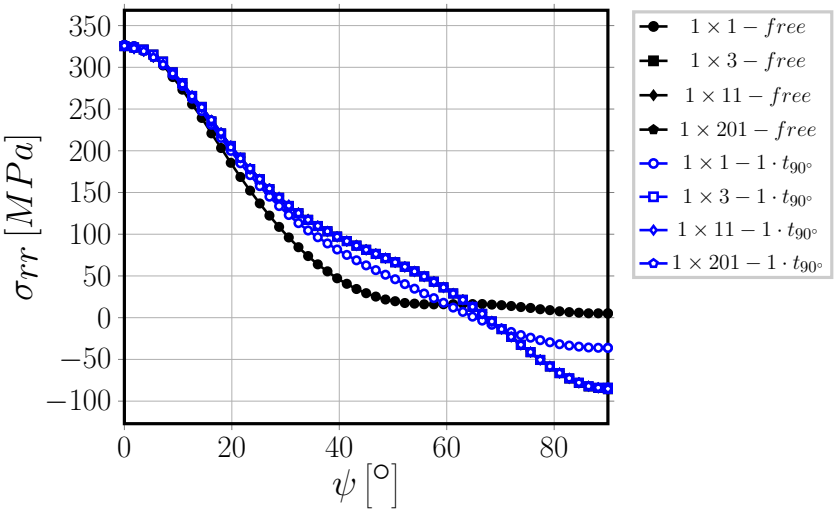


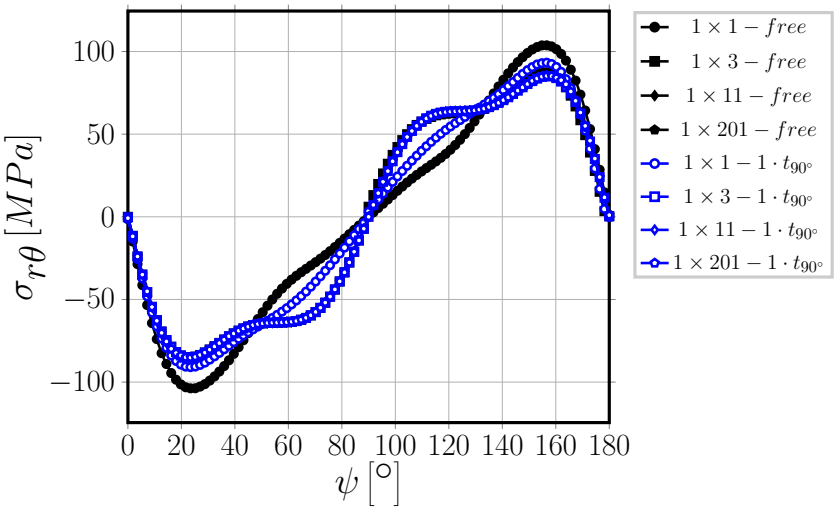


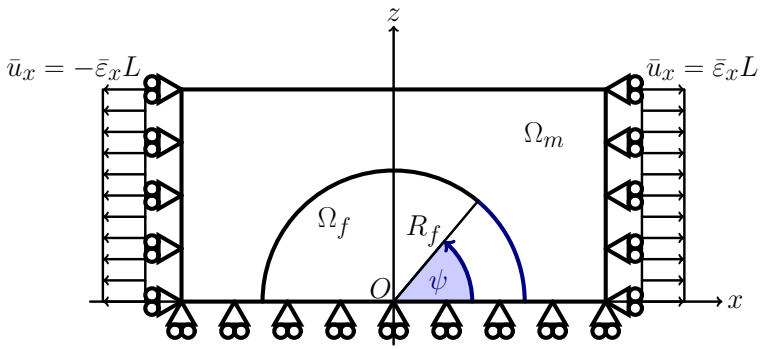

# $\sigma_{rr}$ vs $\tau_{r\theta}$: radial stress vs tangential shear at the interface

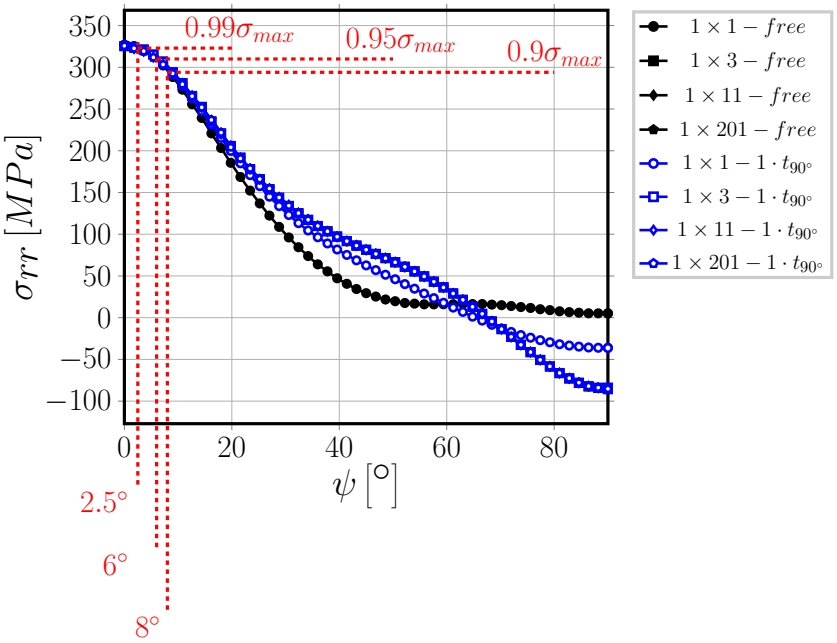


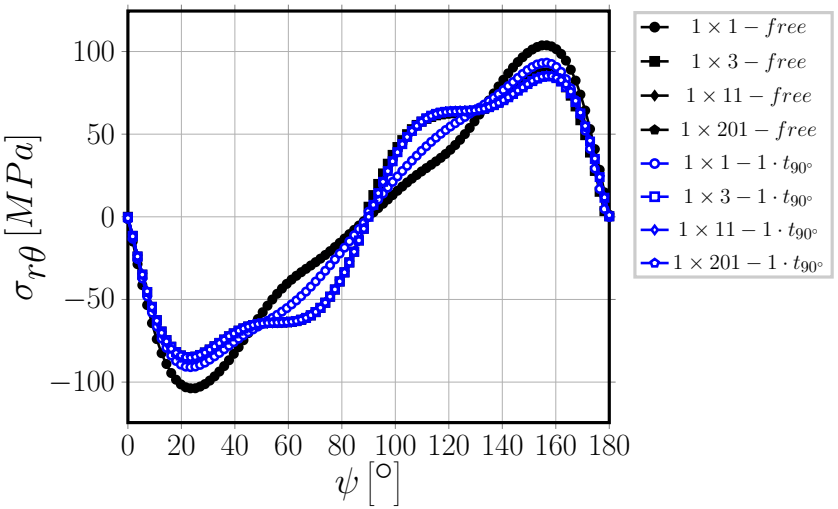


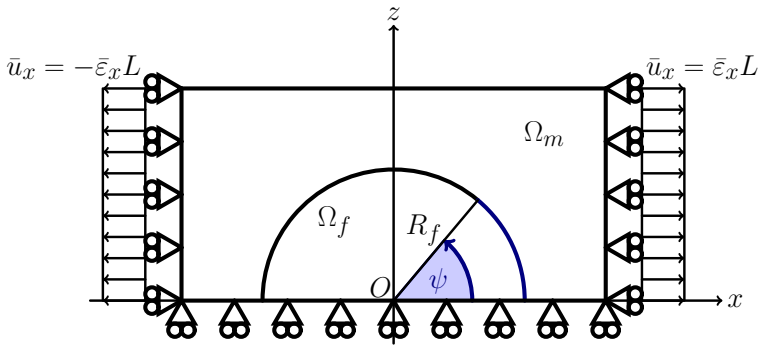

# $\sigma_{LHS}$: local hydrostatic stress at the interface

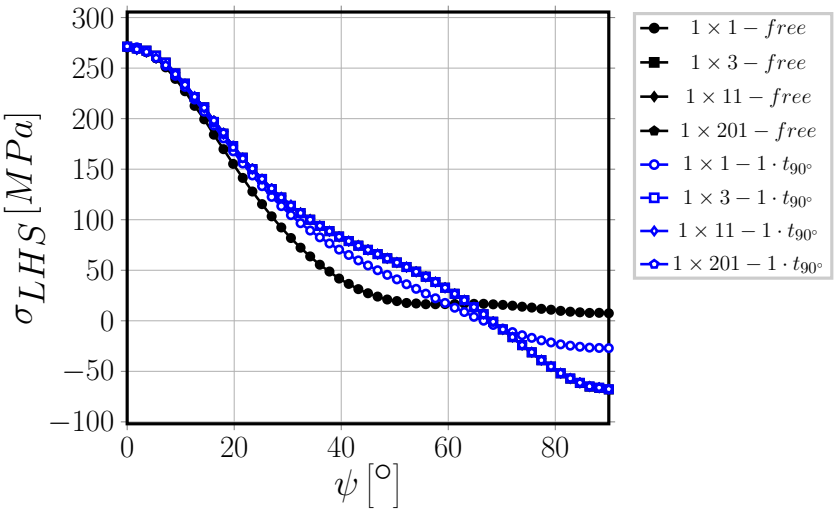


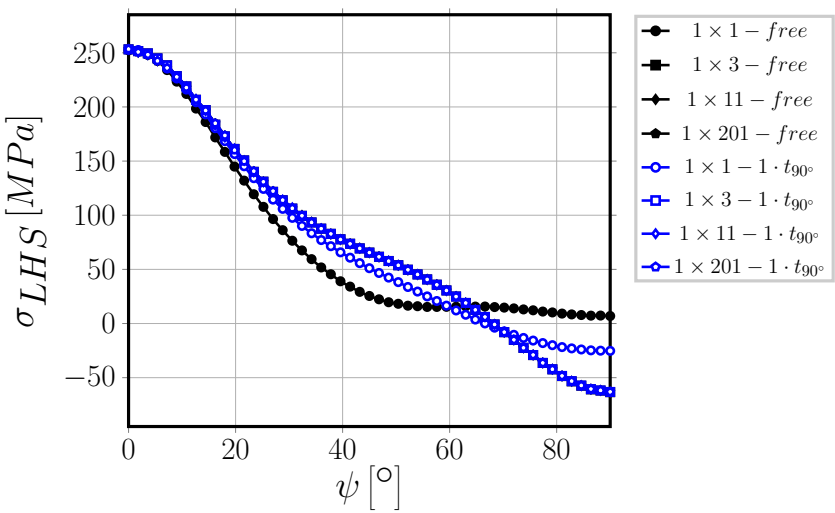


$$\sigma^{2D}_{LHS} = \frac{\sigma_{rr} + \sigma_{\theta\theta}}{2}$$

$$\sigma^{3D}_{LHS} = \frac{\sigma_{rr} + \sigma_{\theta\theta} + \sigma_{yy}}{3}$$

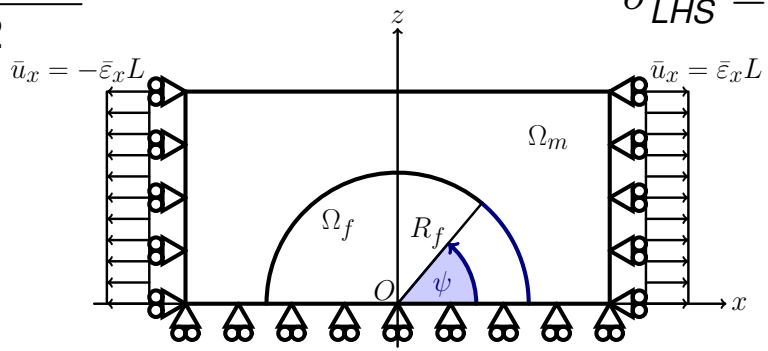

# $\sigma_{LHS}$: local hydrostatic stress at the interface

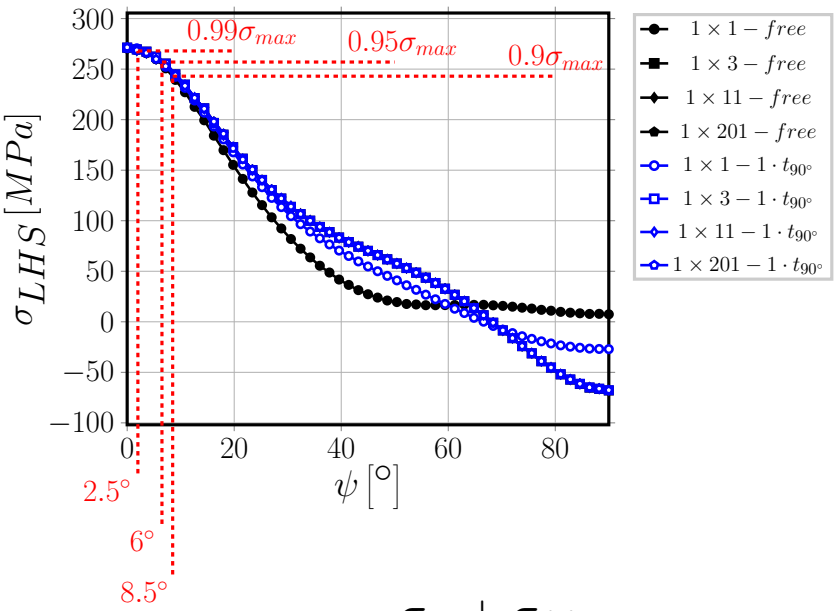


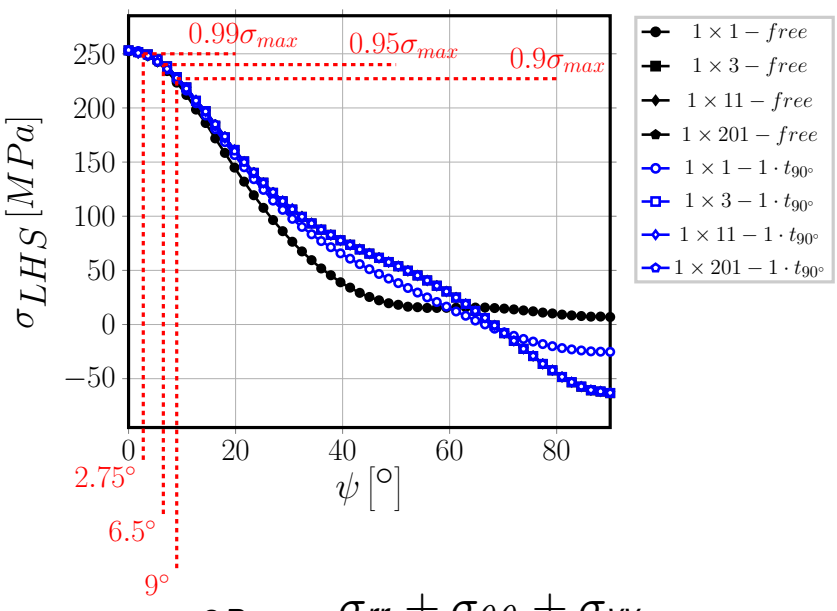


$$\sigma^{2D}_{LHS} = \frac{\sigma_{rr} + \sigma_{\theta\theta}}{2}$$

$$\sigma^{3D}_{LHS} = \frac{\sigma_{rr} + \sigma_{\theta\theta} + \sigma_{yy}}{3}$$

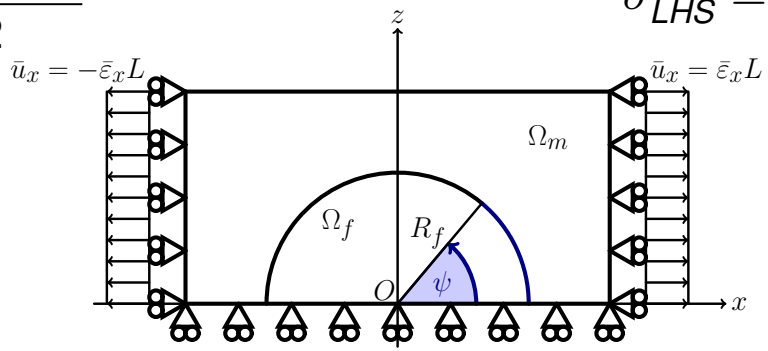

# $\sigma_{vM}$: von Mises stress at the interface

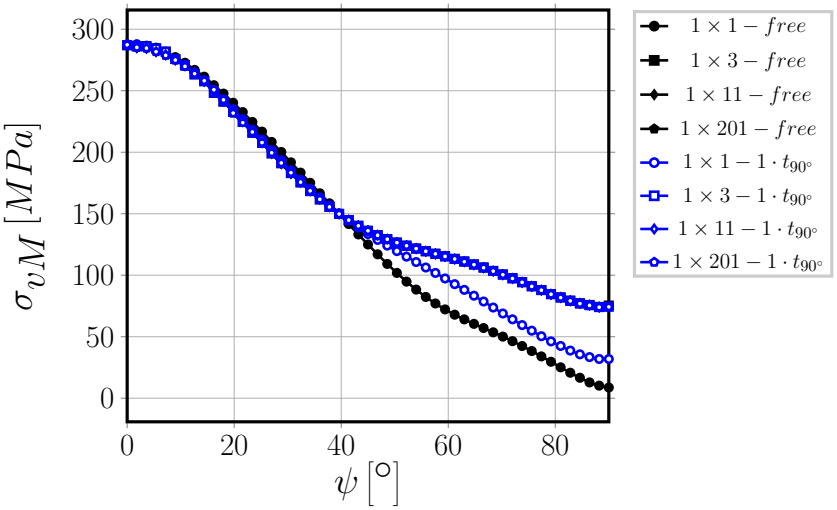


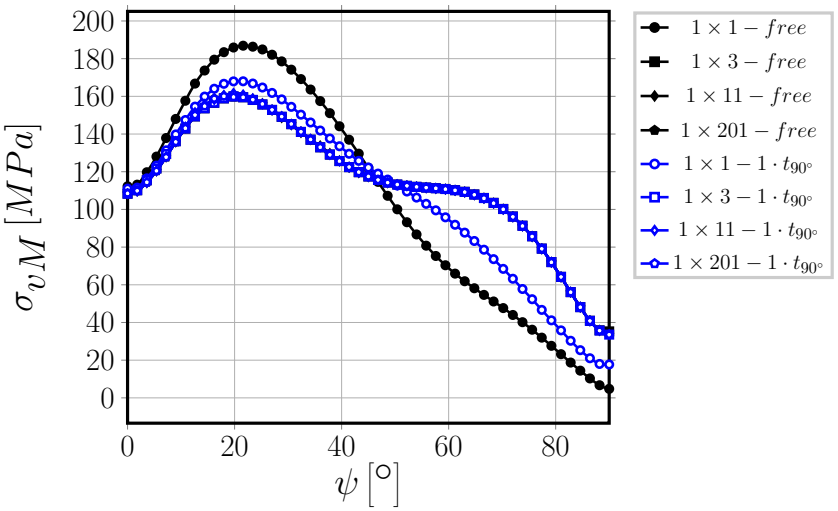


$$\sigma_{vM}^{2D} = \sqrt{(\sigma_{rr} - \sigma_{\theta\theta})^2 + 3\tau_{12}^2}$$

$$\sigma_{LHS}^{3D} = \frac{3}{2} s_{ij} s_{ij} \quad s_{ij} = \sigma_{ij} - \frac{1}{3}\sigma_{kk}\delta_{ij}$$

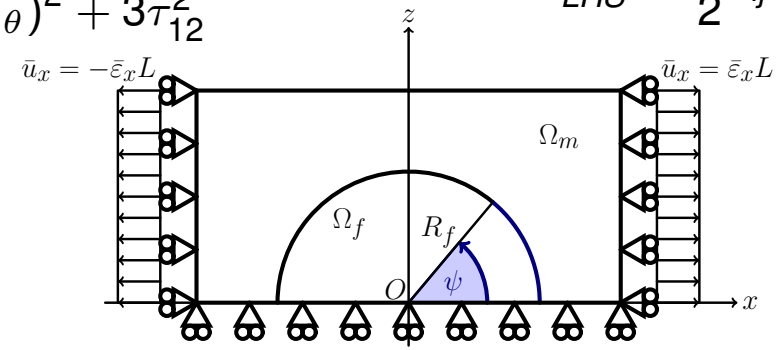

# $\sigma_{vM}$: von Mises stress at the interface

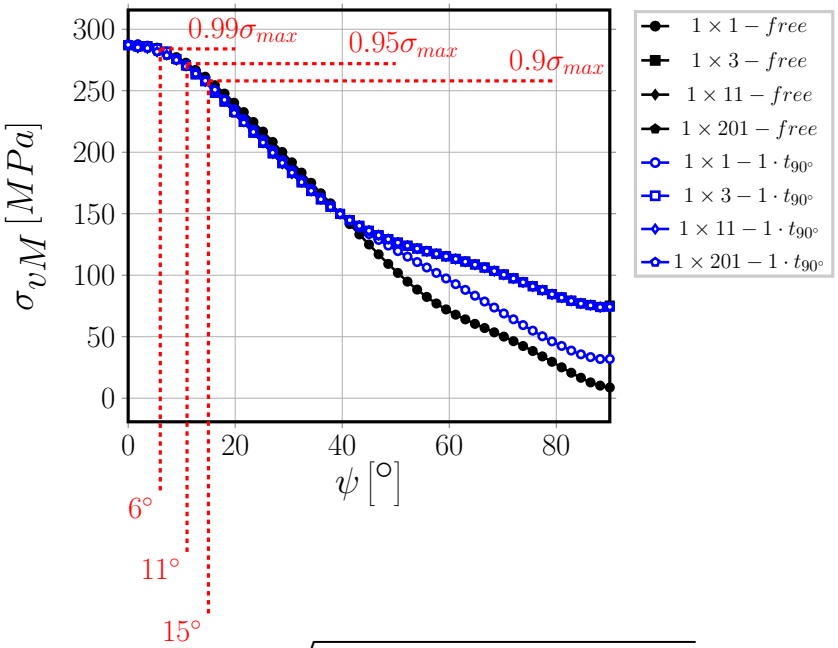


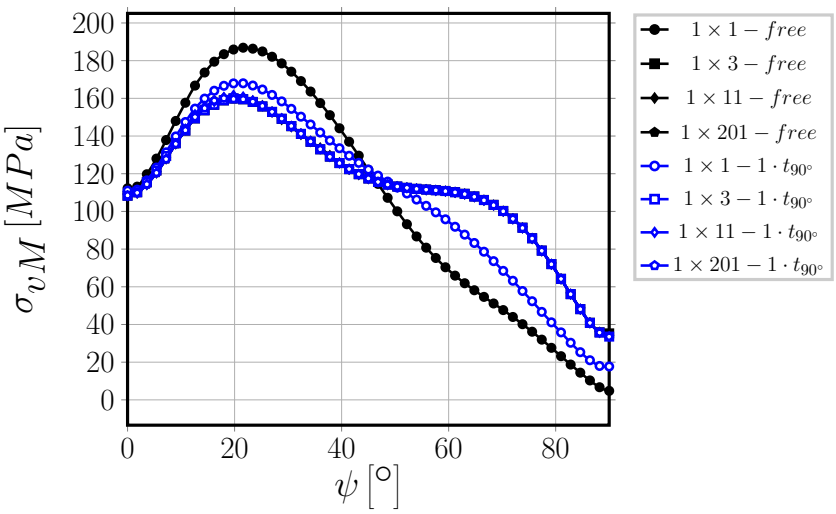


$$\sigma_{vM}^{2D} = \sqrt{(\sigma_{rr}-\sigma_{\theta\theta})^2 + 3\tau_{12}^2}$$

$$\sigma_{LHS}^{3D} = \frac{3}{2} s_{ij} s_{ij} \quad s_{ij} = \sigma_{ij} - \frac{1}{3}\sigma_{kk}\delta_{ij}$$

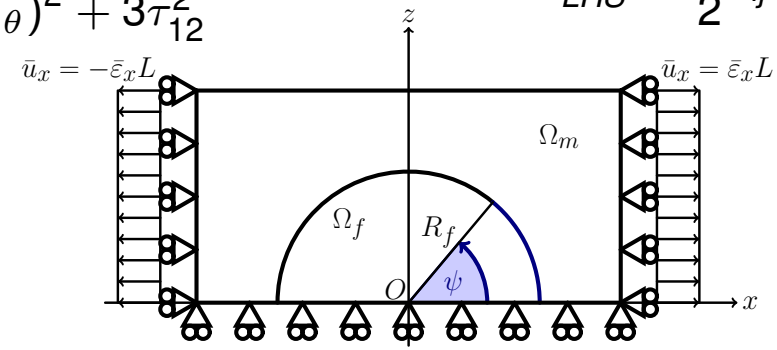

# $\sigma_I$: maximum principal stress at the interface

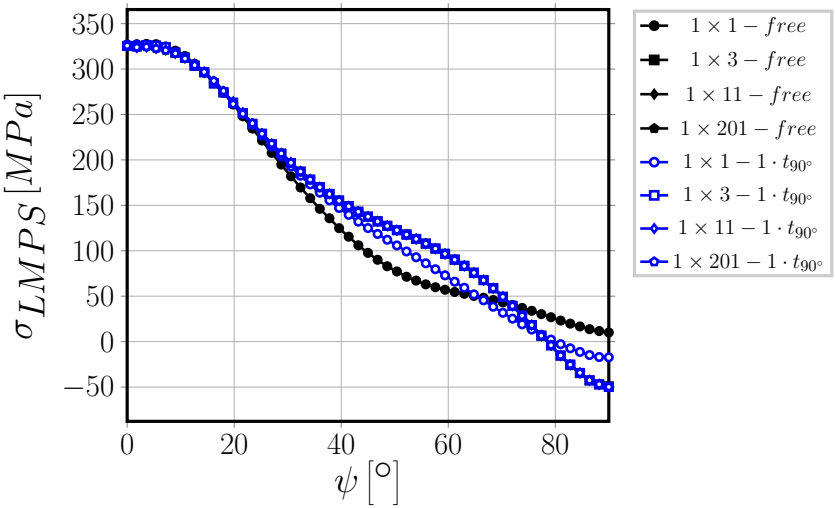


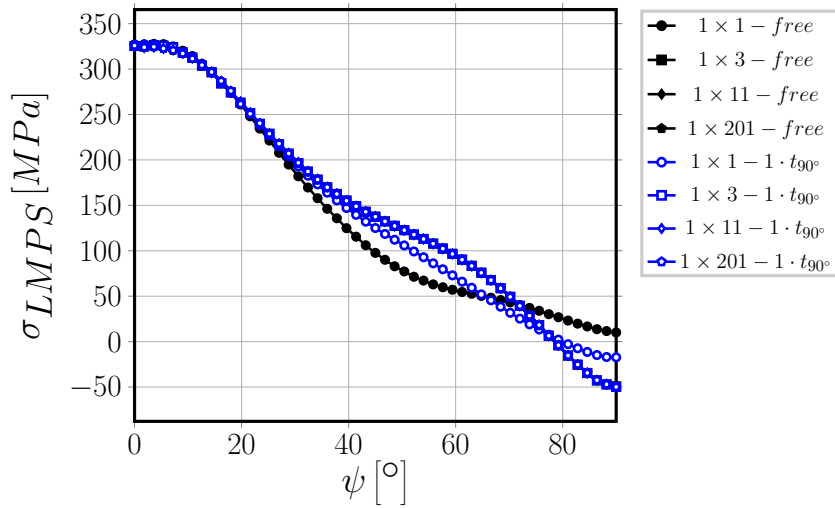


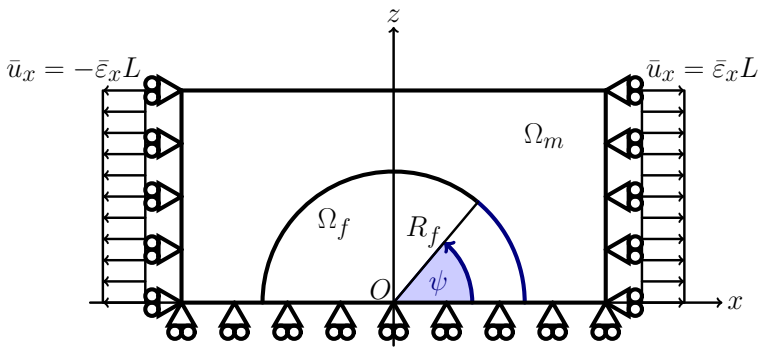

# $\sigma_I$: maximum principal stress at the interface

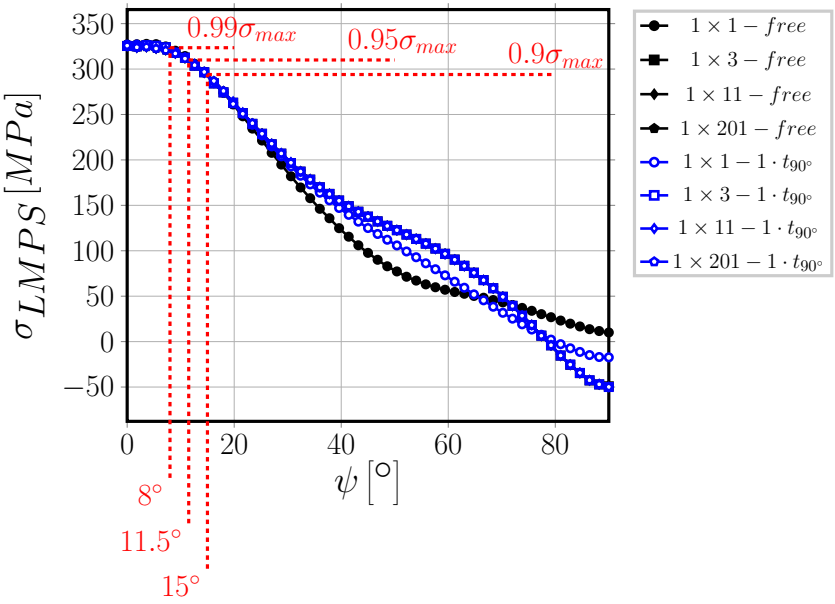


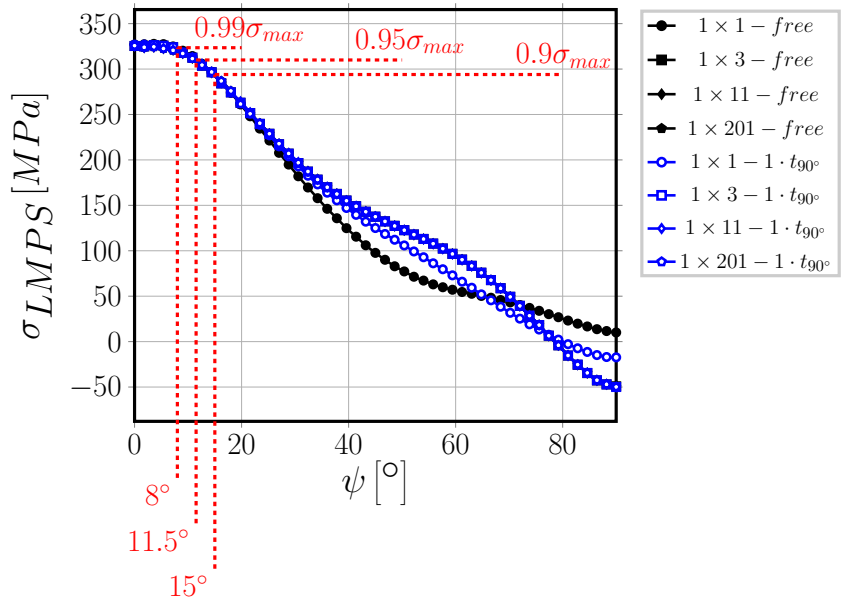


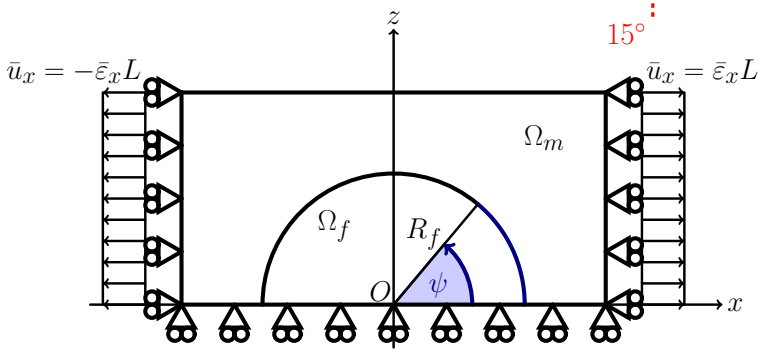

# ↘ Debond Propagation

# Interaction of Debonds: Strain Magnification

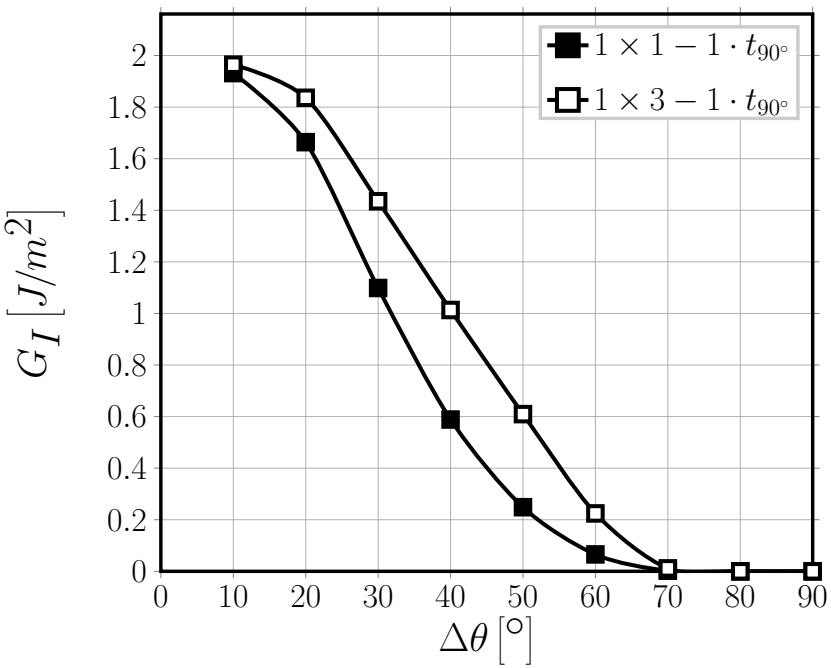


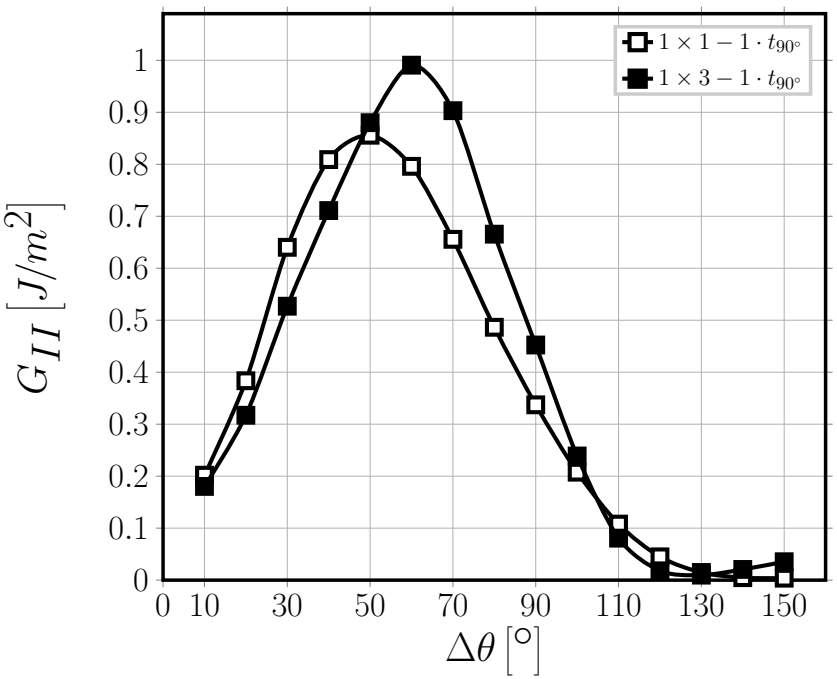


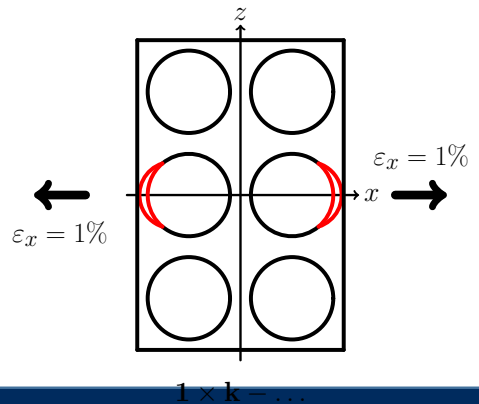

# Interaction of Debonds: Strain Magnification

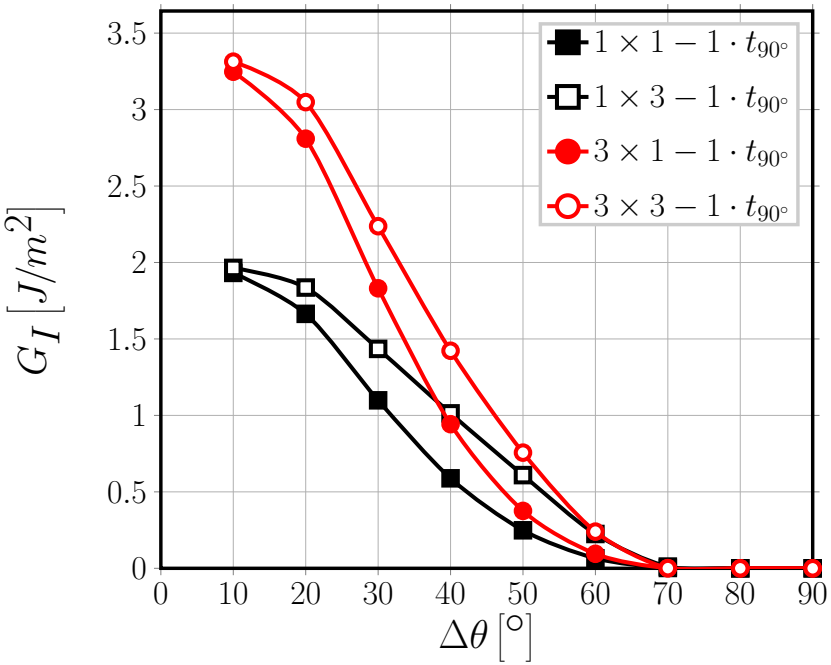


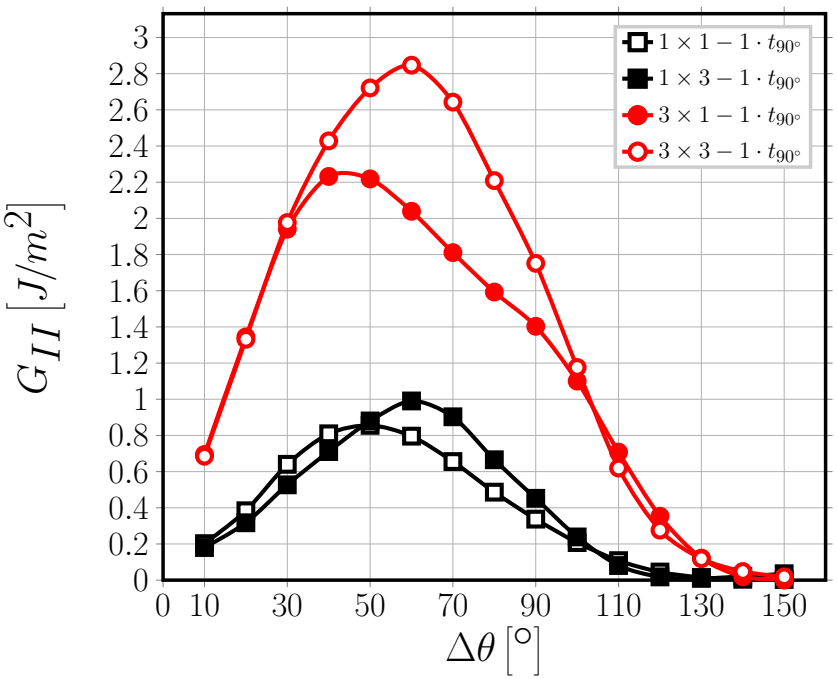


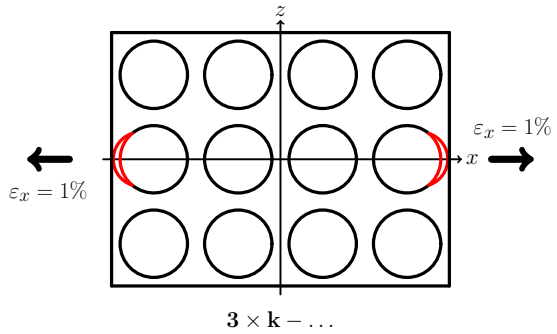

# Interaction of Debonds: Strain Magnification

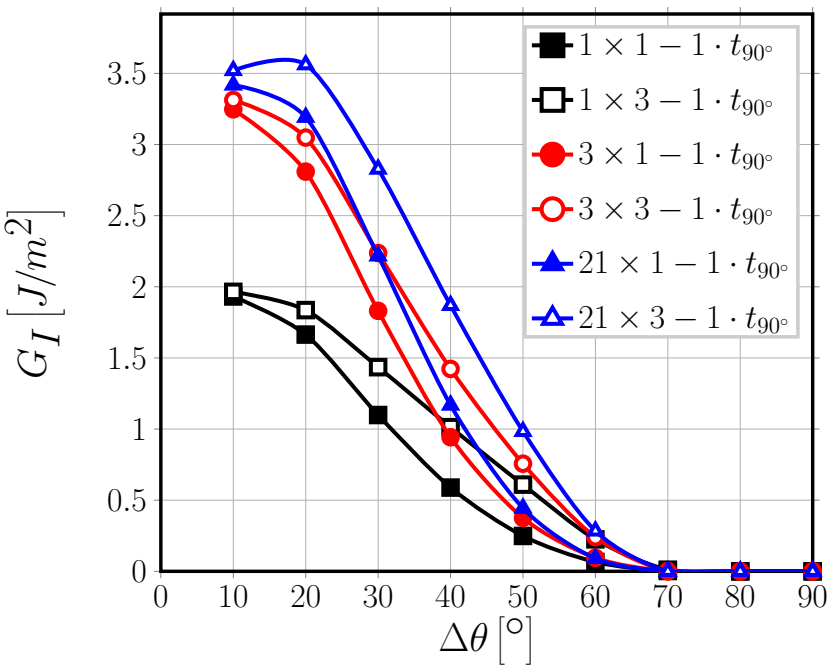


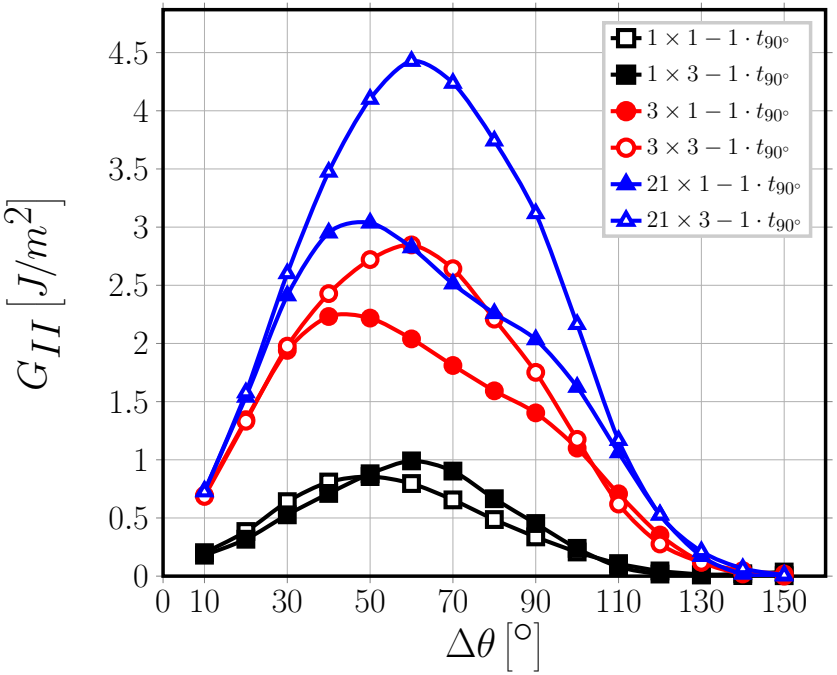


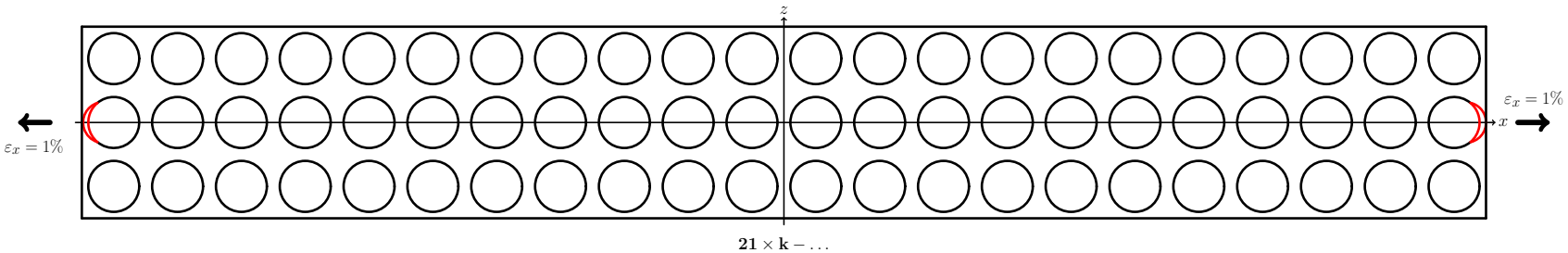

# Interaction of Debonds: Crack Shielding

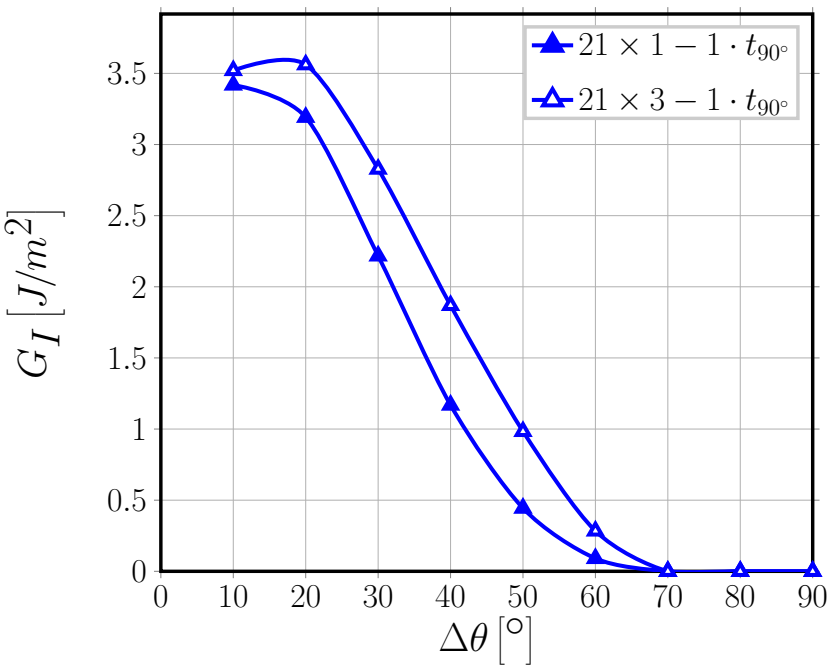


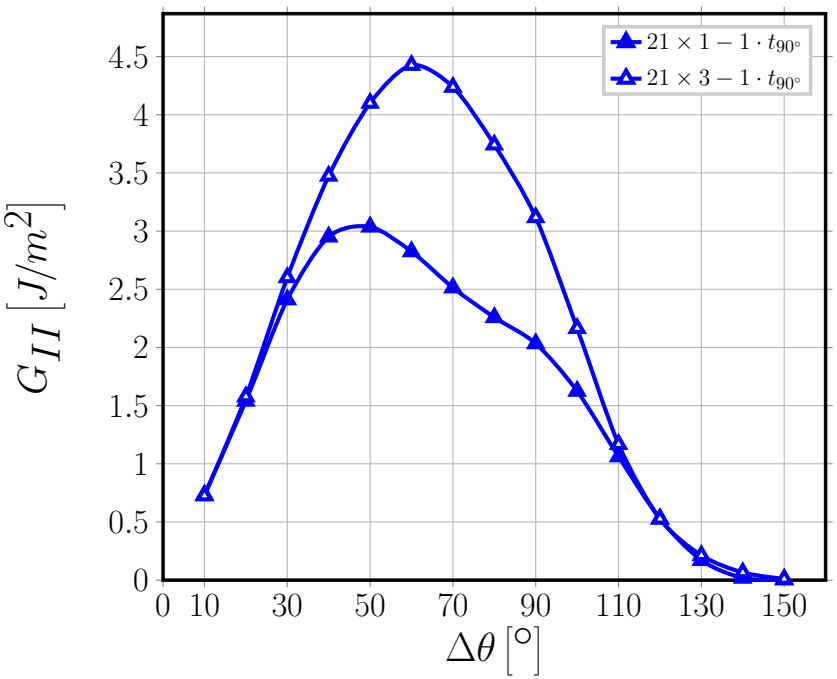


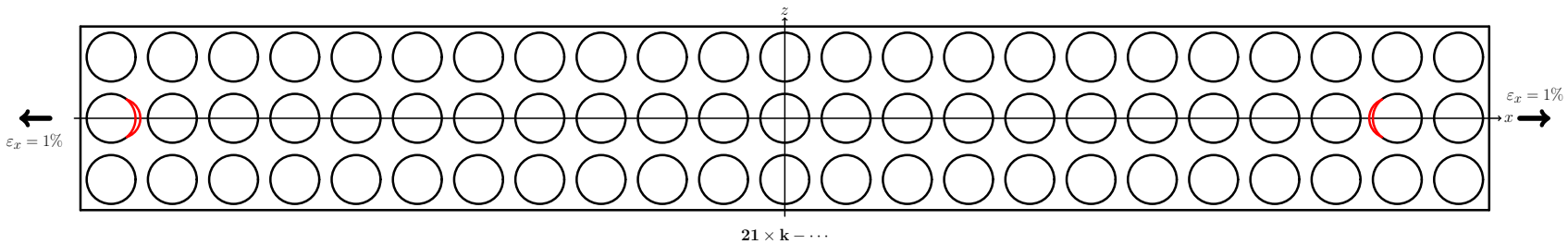

# Interaction of Debonds: Crack Shielding

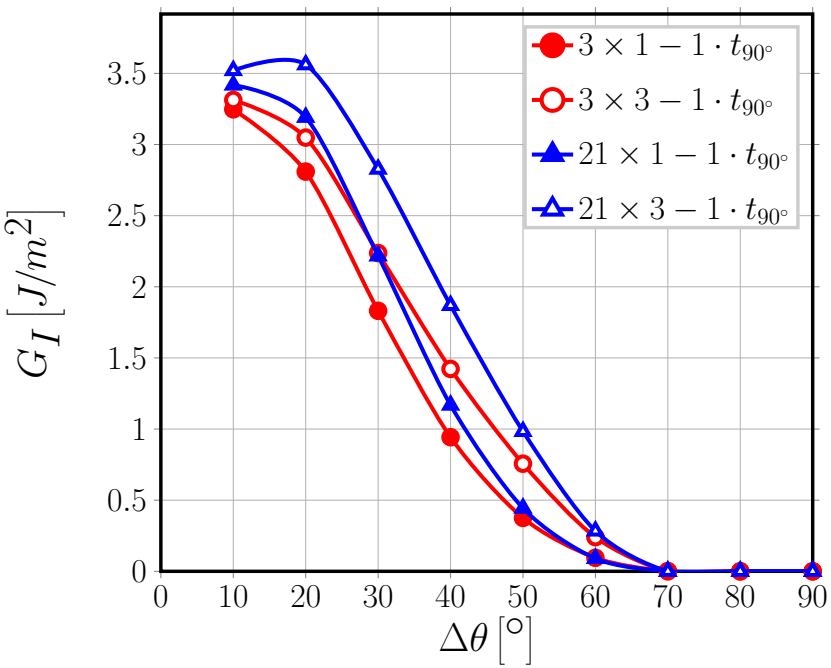


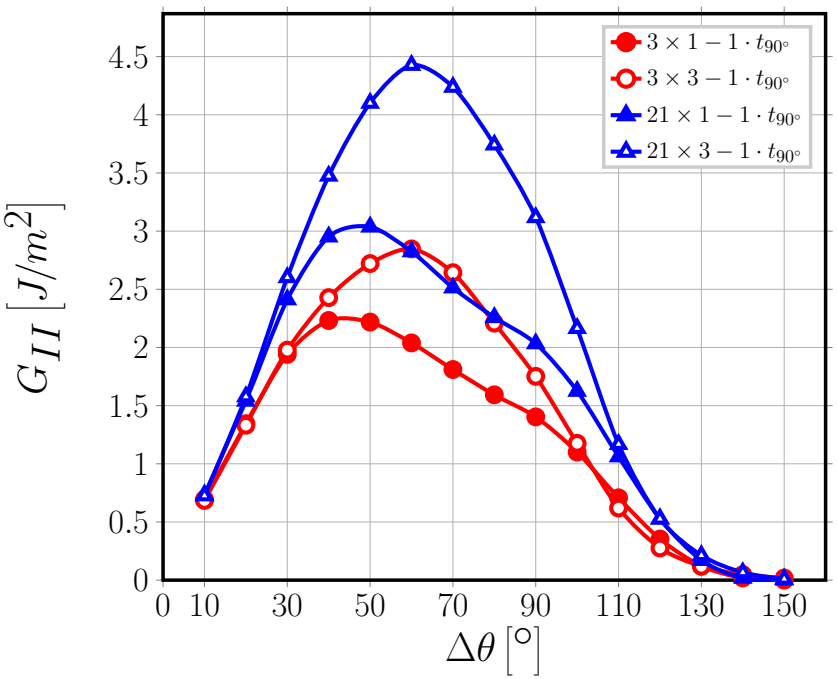


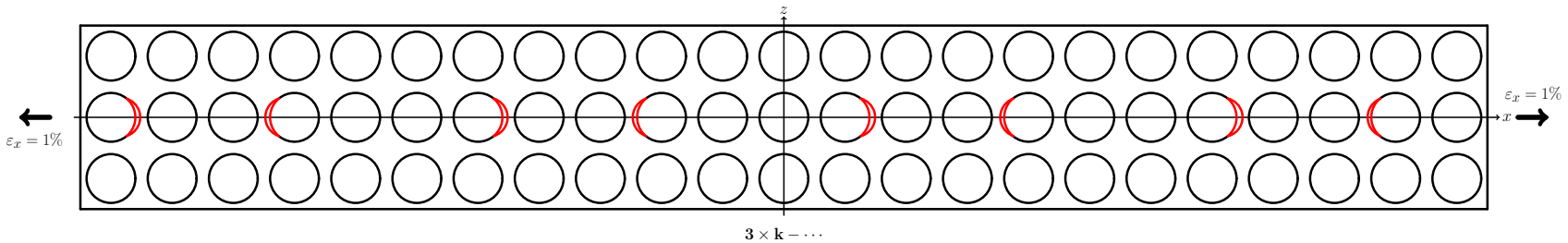

# Interaction of Debonds: Crack Shielding

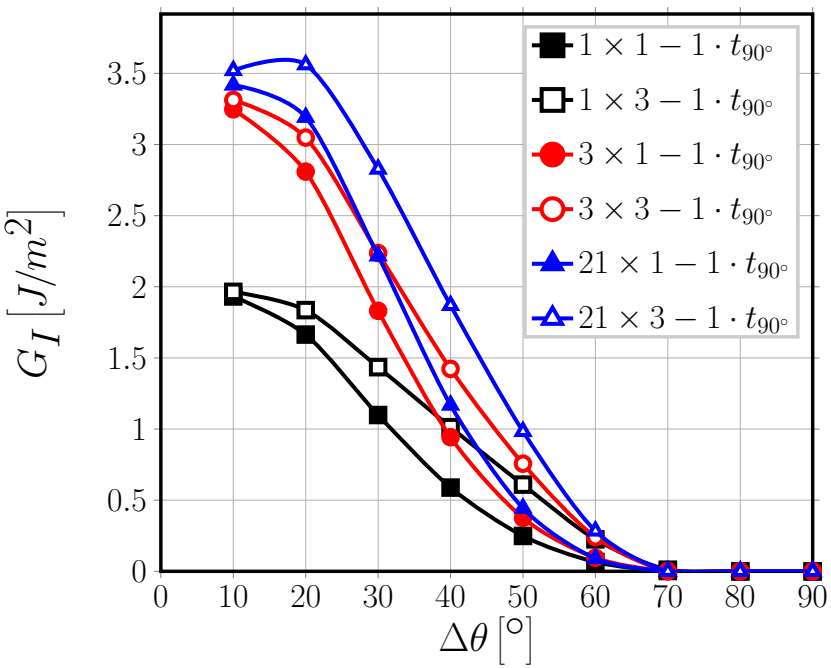


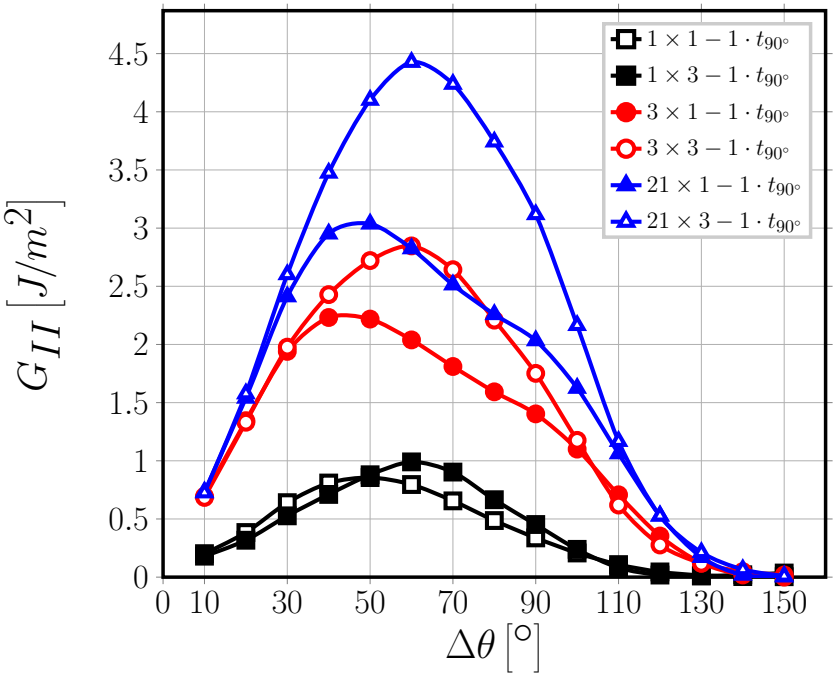


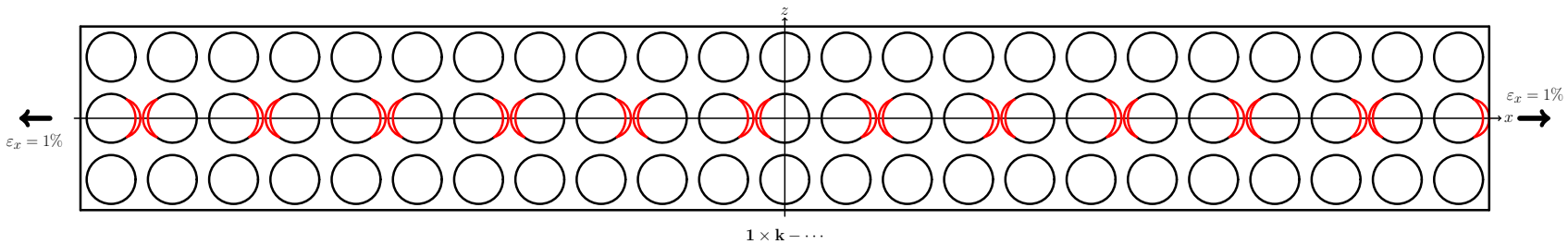

# Effect of 0° ply thickness

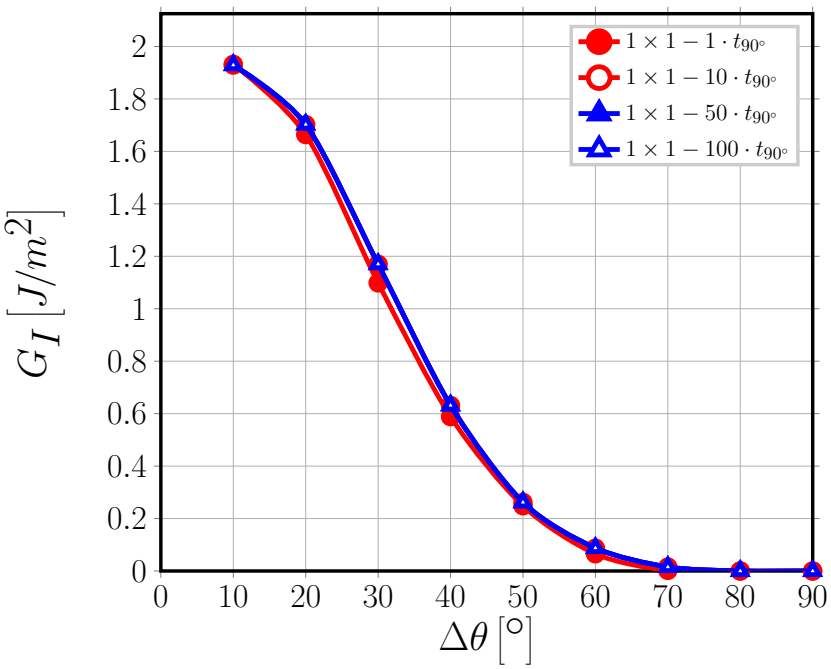


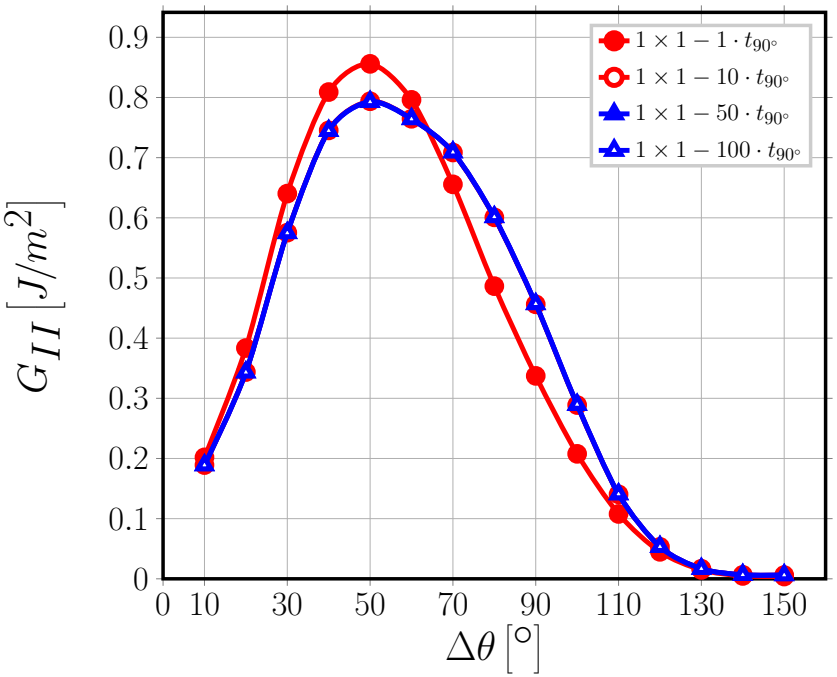


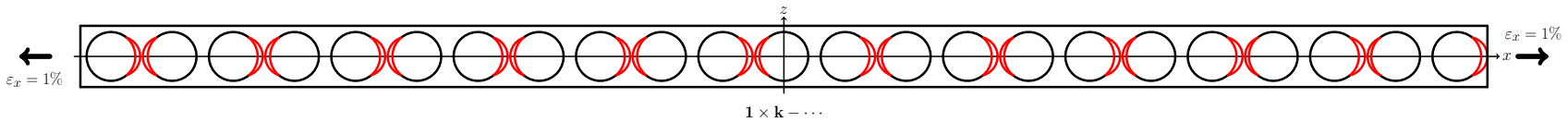

# Effect of 0° ply thickness

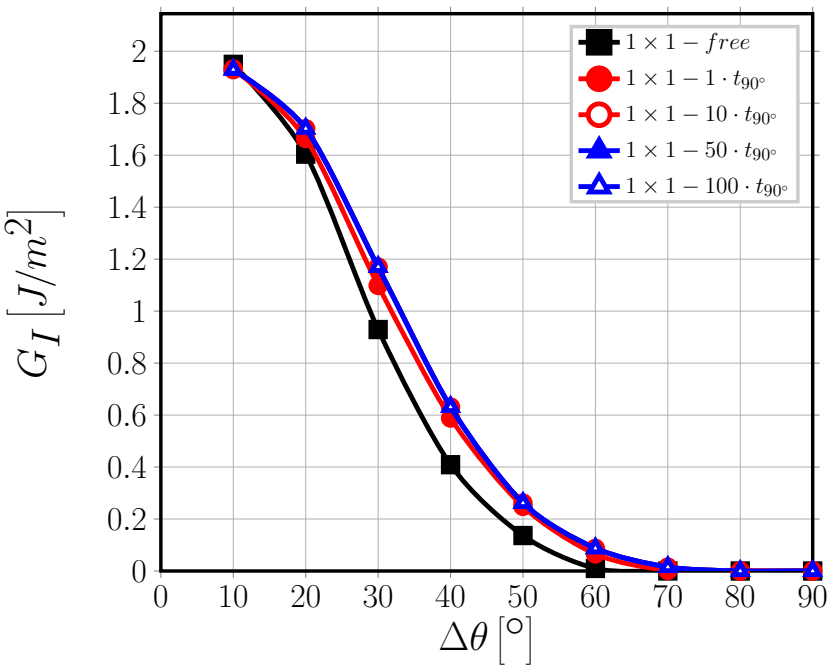


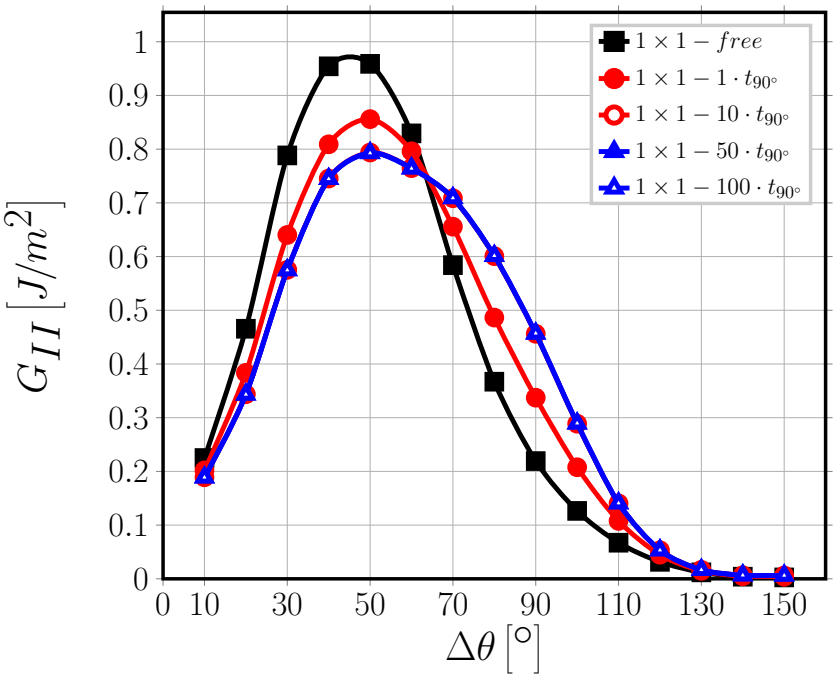


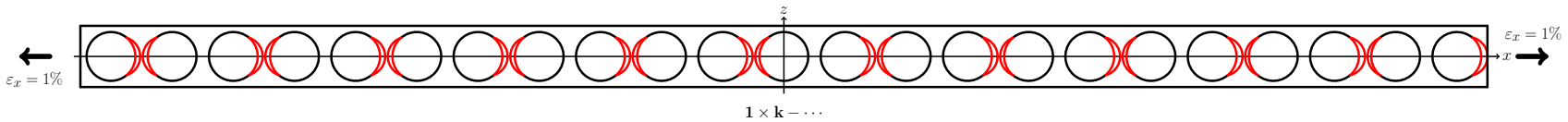

# Effect of 0° ply thickness

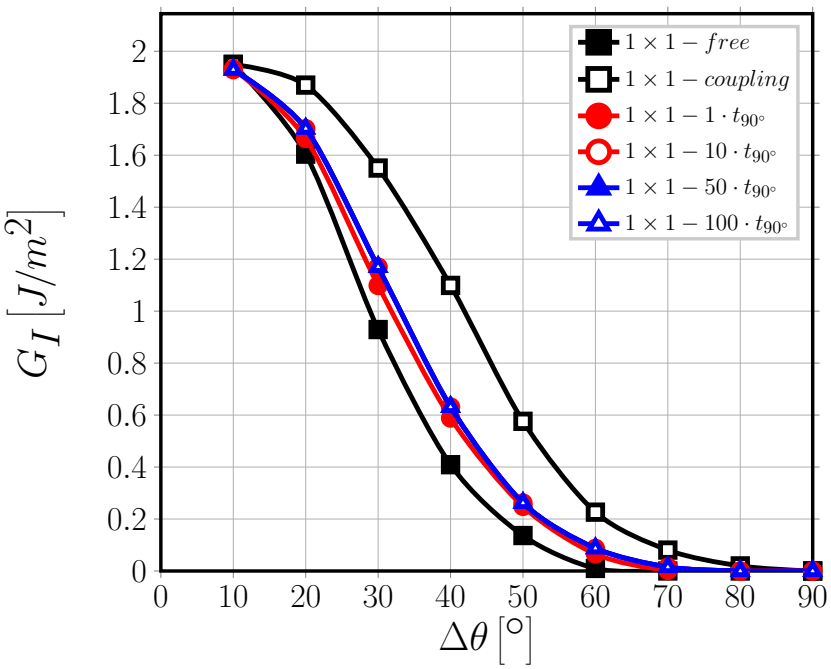


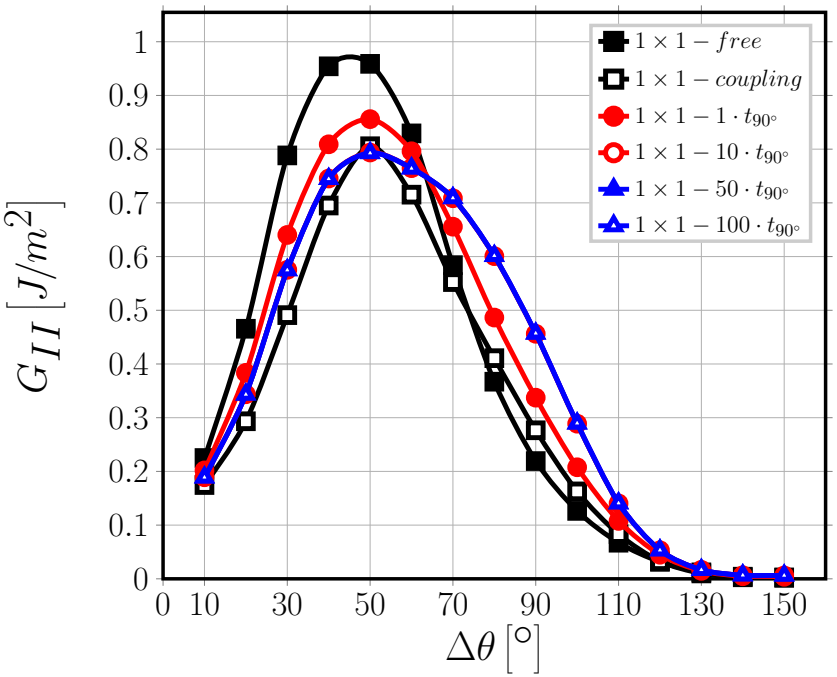


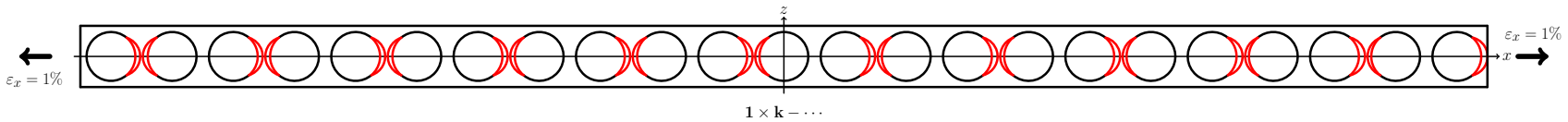

# Effect of 0° ply thickness

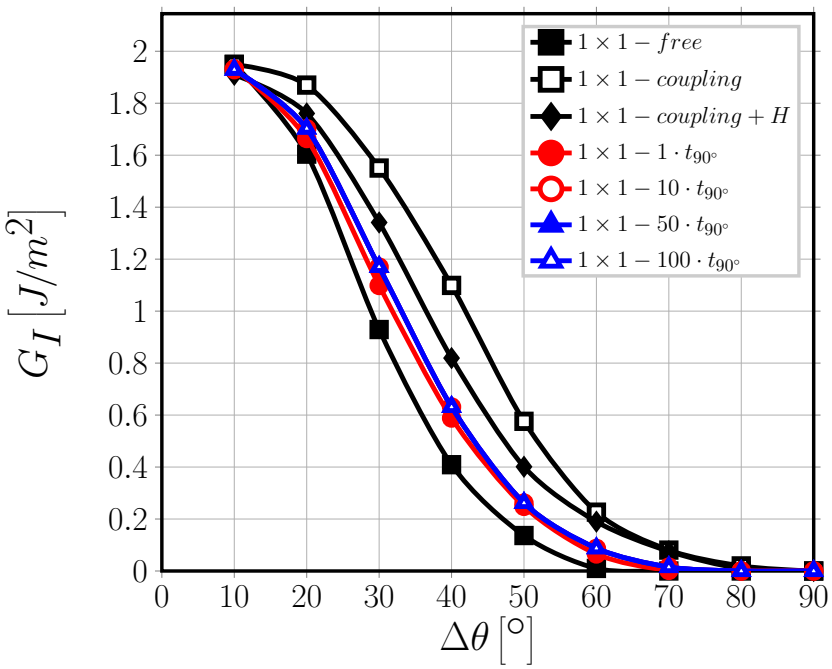


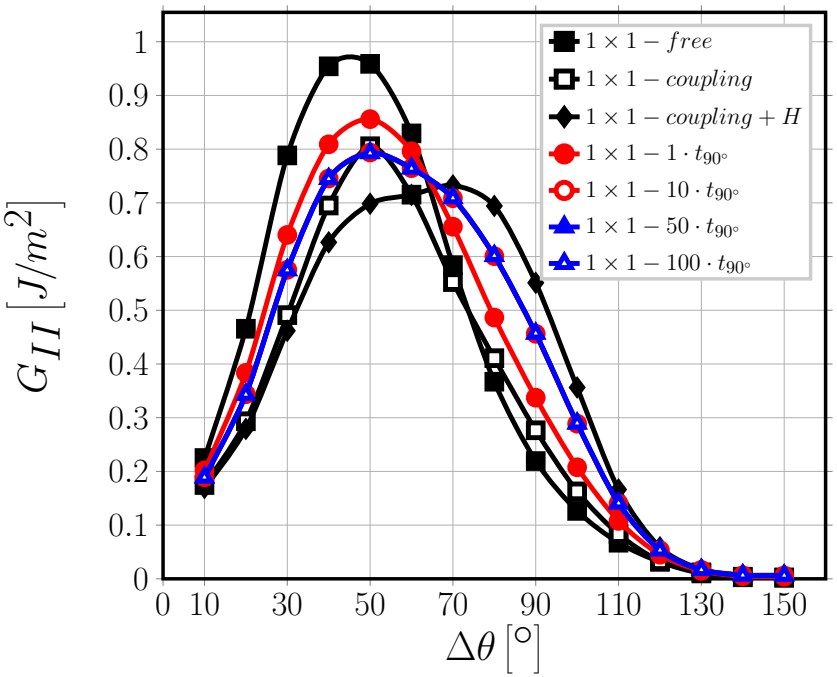


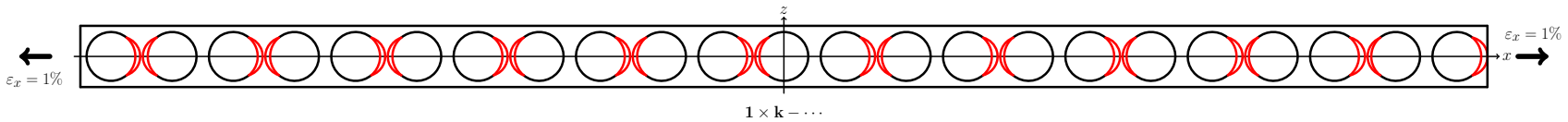

# Effect of 90° ply thickness

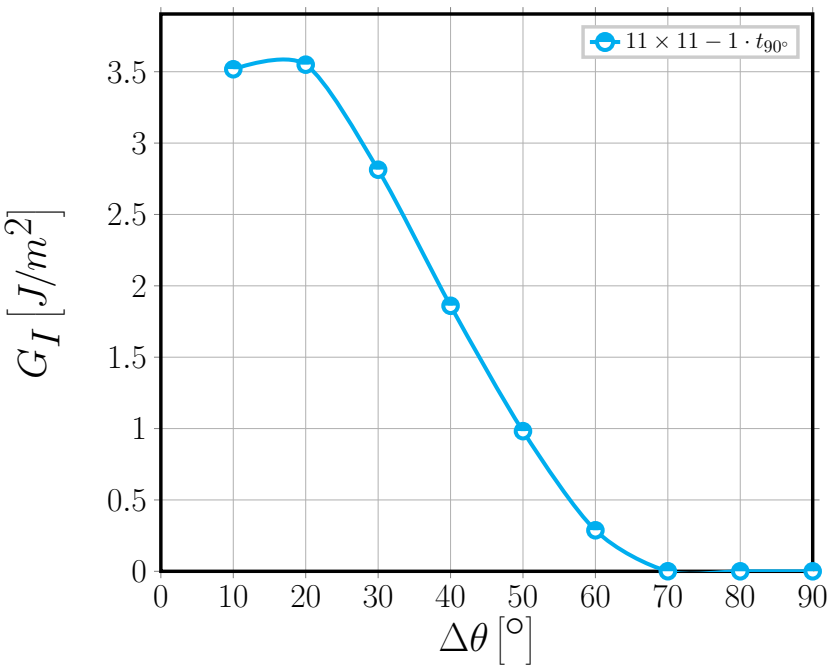


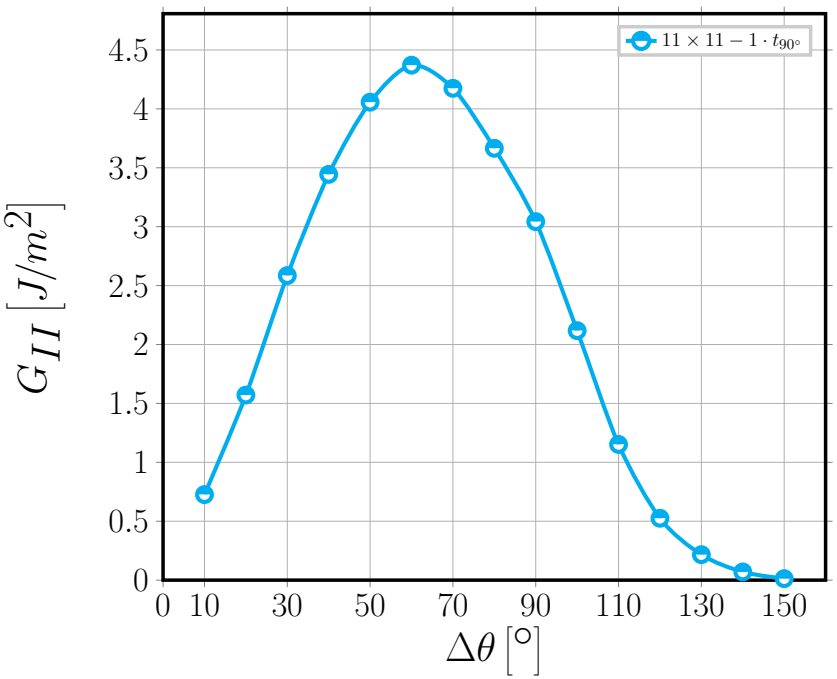


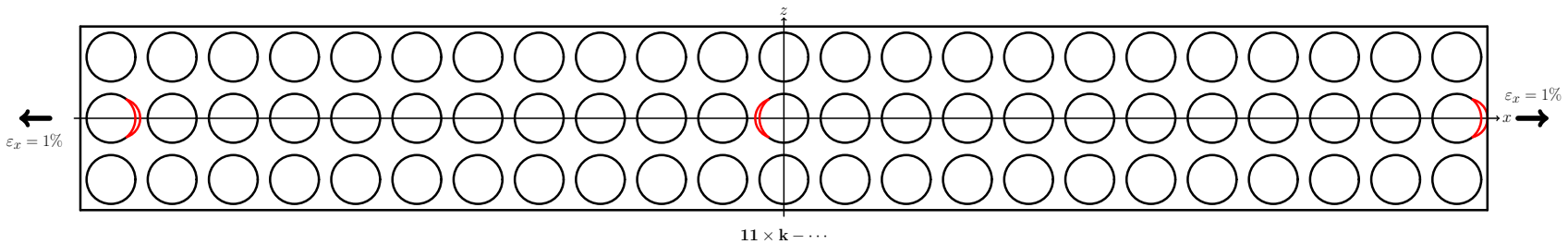

# Effect of 90° ply thickness

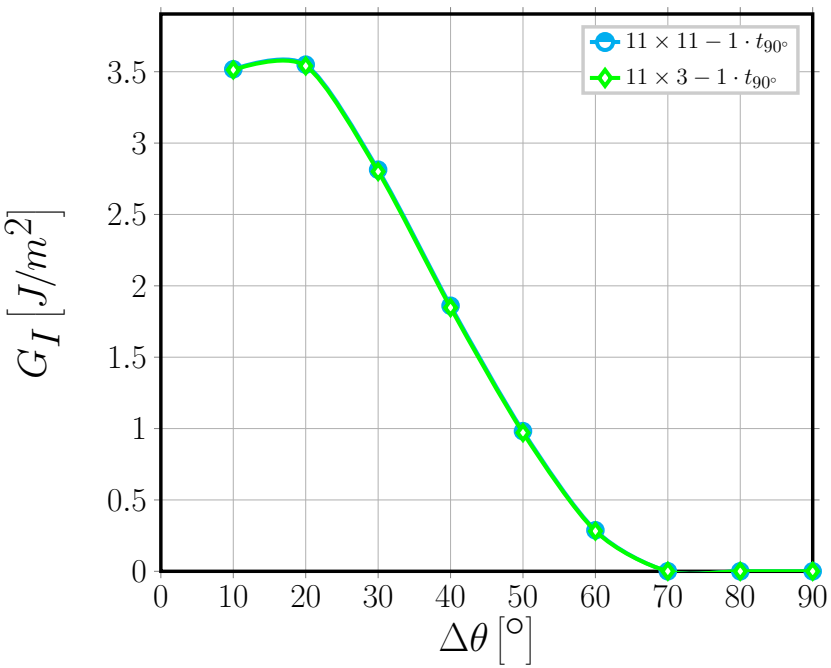


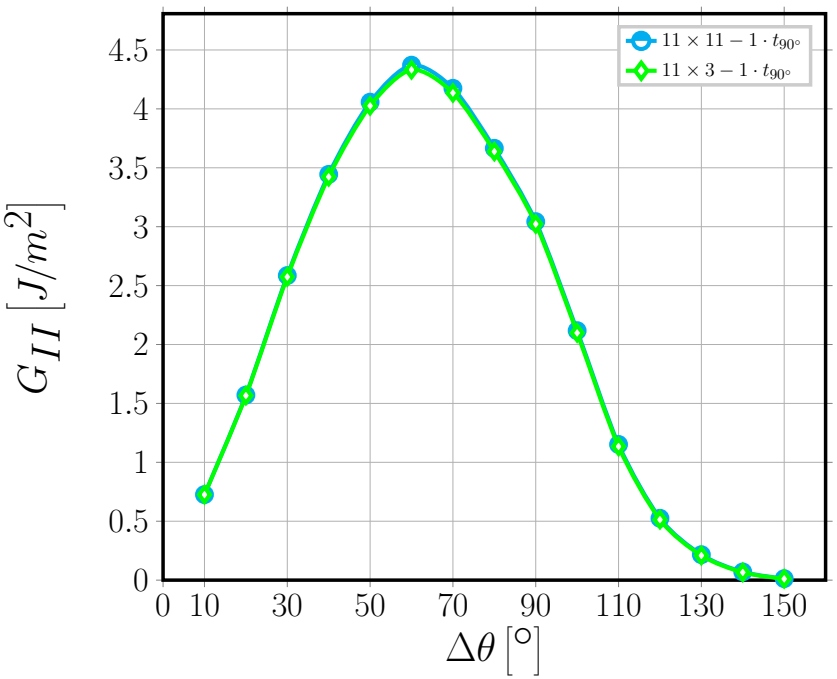


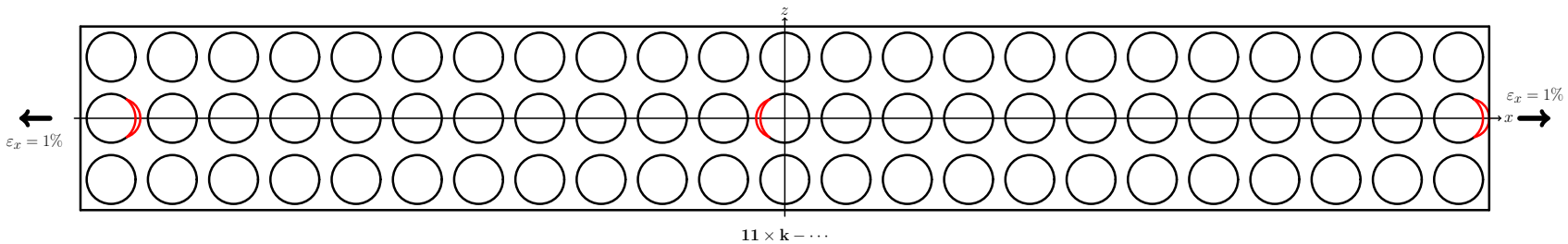

# Effect of 90° ply thickness

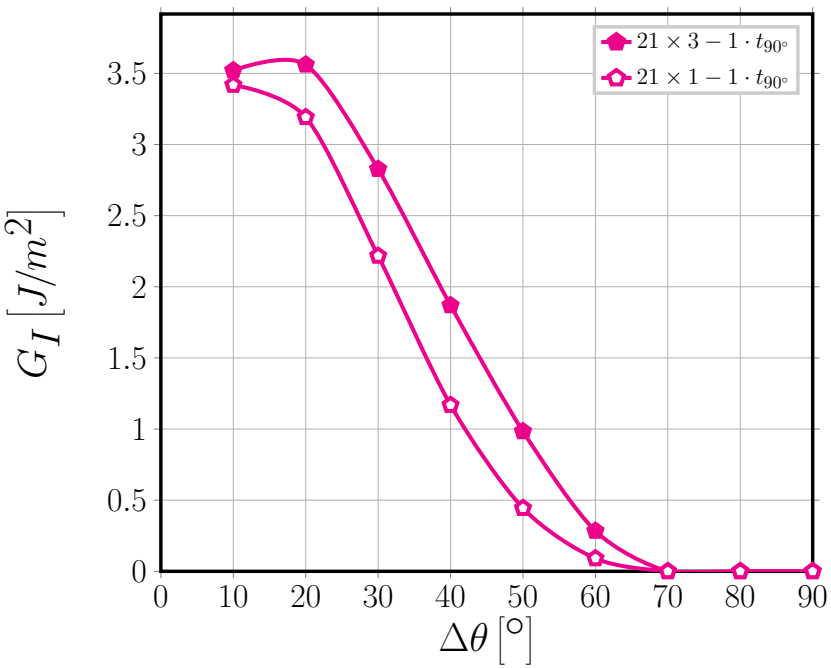


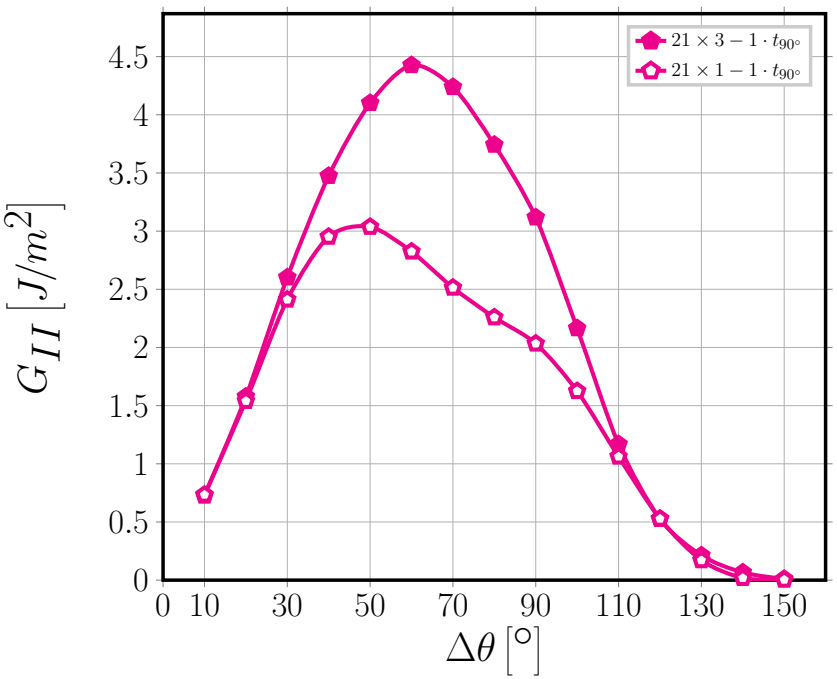


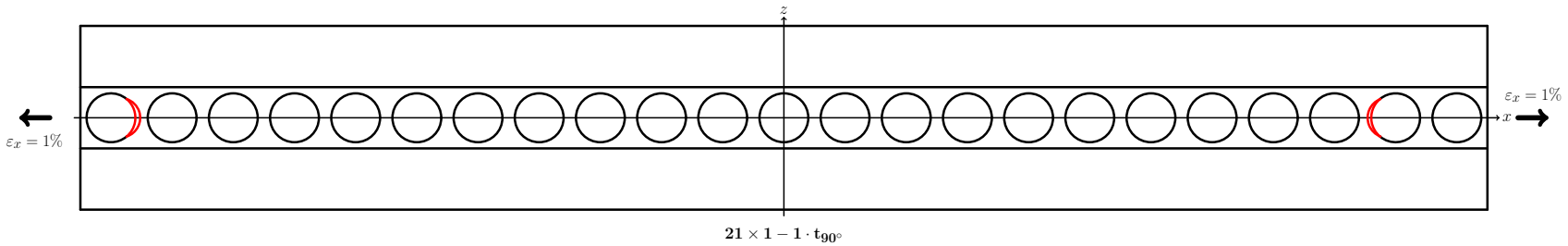

# ↘ CONCLUSIONS

# Conclusions

- ➔ No effect of 90° ply thickness can be observed when $t_{90^\circ}$ is at least $\sim 3\varnothing_{fiber}$
- ➔ Only if $t_{90^\circ}$ is reduced to $1\varnothing_{fiber}$, ERR is reduced for a given level of applied strain, i.e. debond growth is delayed to higher levels of applied strain ($G \sim \varepsilon^2_{applied}$)
- ➔ No effect of 0° ply thickness can be observed when $t_{0^\circ}/t_{90^\circ} > 1$
- ➔ A small difference can be observed when $t_{0^\circ} = t_{90^\circ}$, due to the smaller bending stiffness of a thinner 0° layer


DOC MASE
UNIVERSITÉ DE LORRAINE
EEIGM
LULEÅ UNIVERSITY OF TECHNOLOGY
Education and Culture
Erasmus Mundus